Signal Processing 172 (2020) 107539

Contents lists available at ScienceDirect

Signal Processing

journal homepage: www.elsevier.com/locate/sigpro

Signal detection algorithms for single carrier generalized spatial modulation in doubly selective channels☆

Hamed Abdzadeh-Ziabari*, Benoit Champagne

Department of Electrical and Computer Engineering, McGill University, Montreal, QC, Canada

ARTICLE INFO

Article history:
Received 16 July 2019
Revised 18 December 2019
Accepted 15 February 2020
Available online 20 February 2020

Keywords:
Detection
Doubly selective channels
Interference cancellation
Spatial modulation
Sphere decoding
Tree search

ABSTRACT

This paper is concerned with signal detection for zero-padded single carrier generalized spatial modulation (SC-GSM) in doubly selective channels (DSCs). Novel detection methods are proposed by expressing the DSC in terms of the basis expansion model (BEM) and considering a BEM-based maximum likelihood (BML) framework. The proposed methods, which aim at reducing the complexity of the BML detector, can be divided into two main categories. The methods in the first category, namely BEM-based partial interference cancellation (BPIC) and BPIC with successive interference cancellation (BPIC-SIC), are designed to remove the interference between the signals. Since the satisfactory performance of these methods depend on meeting a constraint on the number of transmit and receive antennas, a second category of methods is proposed, consisting of BEM-based tree search (BTS), BEM-based reduced complexity tree search (BRCTS), and BRCTS with sphere decoding (BRCTS-SD). These methods are developed to overcome the limitations of BPIC and BPIC-SIC while further reducing the detection complexity by shrinking the search space. The performance evaluation of the proposed SC-GSM methods, in terms of computational complexity and bit error rate (BER) over simulated DSCs, underlines their relative merits and clearly demonstrates their advantages over previous methods.

1. Introduction

Spatial modulation (SM), as a multiple-input multiple-output (MIMO) technique in which the antenna indices convey additional information bits, has gained increasing interest over the past few years due to its many advantages such as high spectral\energy efficiency and reduced complexity [1]. By transmitting information through one active antenna at each symbol time, SM provides an innovative solution to overcome the drawbacks of conventional MIMO systems, including inter channel interference, and the need for multiple radio frequency (RF) chains [2] and precise inter antenna calibration/synchronization.

The concept of SM was first introduced in [3,4], where it was proposed that the blocks of information bits be divided into two parts, that is: a first part indicating which antenna should be selected for transmission, and a second part being mapped into a digital symbol taken from a constellation diagram. To reduce the modulation and detection complexity of SM, the space shift keying (SSK) method was proposed in [5] which is based on transmitting information using only antenna indices. The authors in [6] put forward space-time block coded SM (STBC-SM) to benefit from SM along with the decoding simplicity and diversity advantages of space-time block coding (STBC) [7]. In [8] and [9], generalized SM (GSM) was proposed so that the information bits can be transmitted through more than one active antenna. A unified framework was introduced in [10], subsuming different MIMO arrangements including SM, SSK, STBC, linear dispersion codes (LDCs) [11], and Bell Laboratories layered space-time (BLAST) architecture [12], based on selection and linear combination of several linear dispersion matrices.

Most of the methods related to SM and its variants have been proposed and studied under the assumption of slow fading frequency flat channels. Hence, if these methods are to be used in slow fading frequency selective channels, multicarrier modulation techniques such as orthogonal frequency division multiplexing (OFDM), which can transform a wideband frequency selective channel into several narrowband frequency flat channels, must be employed. However, OFDM nullifies most of the advantages of SM due to the need of using multiple RF chains [13–15]. Such practical limitations with OFDM in the context of SM have spurred growing interest toward single carrier (SC) techniques for which the channel can no longer

☆ Part of this work was presented at 2019 IEEE International Conference on Acoustics, Speech and Signal Processing. Funding for this work was provided by a grant from Natural Sciences and Engineering Research Council (NSERC) of Canada (Grant No. NSERC DGDND-2017-00019).

* Corresponding author.
E-mail addresses: hamed.abdzadehziabari@mail.mcgill.ca (H. Abdzadeh-Ziabari), benoit.champagne@mcgill.ca (B. Champagne).

https://doi.org/10.1016/j.sigpro.2020.107539
0165-1684/

be considered frequency flat, and inter-symbol interference (ISI) exists [13–16].

In frequency selective channels, SC-SM based techniques such as SC-GSM are confronted with inter-block interference (IBI), which can be avoided using cyclic prefix (CP) or zero-padding. It has been shown that, compared with CP, zero-padding has the advantages of achieving full multipath diversity and lower bit error rate (BER) [14,17]. Hence, we will focus on zero-padded SC-SM based techniques in this paper.

From the viewpoint of signal detection for SC-SM based techniques, only a few works have considered slow fading frequency selective channels. Methods based on partial interference cancellation (PIC) and PIC with successive interference cancellation (PIC-SIC) were proposed in [17] for SC-SM. The authors in [18] exploited the structure of the channel matrix in order to reduce the complexity of SC-SM signal detection. Tree-search based methods with the goal of reducing the size of the search space using either the minimum values of a certain cost function or sphere decoding, were respectively advanced in [19] and [20] for SC-GSM.

Besides frequency selectivity, time selectivity in which the properties of the radio channels undergo significant changes over relatively short time intervals, is a distinguishing characteristic of many wireless communication channels. Doubly selective channels (DSCs), which exhibit both frequency and time selectivity, are encountered in many applications involving high-rate transmission over mobile environment, such as in high speed train communications [21], underwater acoustic communications [22], digital video broadcasting (DVB), and next generation cellular systems [23].

Due to the fast variations of the DSC properties over both the frequency and time dimensions, communication systems operating under such conditions, whether they be SC or multi-carrier based, experience high conditions of interference in the time and frequency domains. In general, operation in a DSC significantly alters or degrades the performance of a communication system designed purely on the basis of a single type of selectivity.

Several methods have been proposed in the literature to cope with equalization and detection by exploiting the basis expansion model (BEM) for DSC representation. In [24], the minimum MSE decision feedback equalizer is proposed for single-input multiple-output (SIMO) systems. The work in [25] deals with time- and frequency-domain per-tone equalization for OFDM systems. A time-varying finite impulse response equalizer is designed for SIMO systems in [26]. The authors in [27] have developed a scheme for product-convolution decomposition for equalization in OFDM systems. In [28], an algorithm based on the variational Bayesian inference framework is proposed for signal detection for OFDM-based virtual MIMO. The concept of virtual trajectory (VT) reception is presented for MIMO-OFDM systems in [29].

To the best of our knowledge, on the one-hand, none of the BEM-based methods for DSC are developed for SC-GSM signal detection, and none can be directly applied or extended to solve this problem. Some of these methods do not consider a MIMO system, while the others are mainly developed for MIMO OFDM systems and not SC systems; in any case, they do not exploit the spatial structure of the GSM signal. On the other hand, none of the previous works related to SC-GSM and its variants have addressed signal detection under the challenging conditions in DSCs.

In this paper, we bridge this gap by proposing novel methods for detection of zero-padded SC-GSM signals in DSCs. We represent the radio channel by means of the basis expansion model (BEM), which provides the most accurate approximation of a DSC [27]. First, the BEM-based maximum likelihood (BML) detector, which has many desirable properties but is yet impractical due to its high complexity, is presented as an underlying framework. Next, different categories of reduced complexity methods are proposed. The methods belonging to the first category, i.e. BEM-based PIC (PBIC) and BEM-based PIC-SIC, rely on removing the interference between the signals. The methods in the second category, i.e. BEM-based tree search (BTS), BEM-based reduced complexity tree search (BRCTS), and BRCTS with sphere decoding (BRCTS-SD), aim at shrinking the search space. These methods have lower complexity and do not impose a constraint on the numbers of transmit and receive antennas, as seen in BPIC and BPIC-SIC. The performance of the proposed methods is assessed in terms of computational complexity and simulated BER under representative DSC conditions. In addition to offering a convenient trade-off between complexity and BER, it is shown that the proposed methods can achieve remarkably better performance in comparison with previous methods.

It is worth mentioning that this paper builds on our recently published conference paper [30]. In comparison with [30], the new work has the following novelties. First, in [30], we considered signal detection for SM, whereas the current work deals with signal detection for GSM. Second, in this paper, we have proposed three new methods, namely, BTS, BRCTS, and BRCTS-SD that overcome the limitations of the BPIC and BPIC-SIC methods in [30] while further reducing the complexity. Finally, this paper provides a thorough performance evaluation in terms of complexity and BER.

The rest of the paper is organized as follows. Section 2 presents the system model including the BEM. The proposed BML detector along with the proposed BPIC and BPIC-SIC methods are presented in Section 3. The proposed tree search-based methods are developed in Section 4. The performance evaluation of the new methods is addressed in Section 5. Finally, Section 6 concludes the paper.

2. System model

A SC-GSM system is considered with N_T transmit and N_R receive antennas, where N_a transmit antennas are active during signal transmission at each time interval. The input data are divided into blocks of KB bits where K is the number of GSM symbols in each SC-GSM block and B information bits are conveyed in each GSM symbol. Out of these B bits, $\lfloor \log_2 \binom{N_T}{N_a} \rfloor$ bits are used to identify the active antennas, where $\lfloor \cdot \rfloor$ and $\binom{N_T}{N_a}$ denote the floor function and the binomial coefficient, respectively. The remaining $\log_2 \zeta$ bits are mapped to N_a symbols $s_{k,0}, s_{k,1}, \cdots, s_{k,N_a-1}$ belonging to a signal constellation, where ζ represents the size of the constellation and $s_{k,m}$ denotes the mth symbol at the kth time interval[1] Thus, the GSM symbol sent out from the N_T transmit antennas at the kth time interval can be written in vector form as

$$\mathbf{s}_k = [\cdots, 0, s_{k,0}, 0, \cdots, 0, s_{k,1}, 0, \cdots, 0, s_{k,N_a-1}, 0, \cdots]^T \in \mathbb{C}^{N_T \times 1}, \tag{1}$$

where $(\cdot)^T$ denotes the transpose operation. A SC-GSM block of data is then formed by stacking the GSM symbols followed by zero-padding as

$$\mathbf{S} = [\underbrace{\mathbf{0}_{N_T\times 1}, \cdots, \mathbf{0}_{N_T\times 1}}_{K_G}, \mathbf{s}_0, \mathbf{s}_1, \cdots, \mathbf{s}_{K-1}] \in \mathbb{C}^{N_T \times (K+K_G)}. \tag{2}$$

where $\mathbf{0}_{N_T\times 1} \in \mathbb{R}^{N_T\times 1}$ denotes an all zero vector, and K_G is the number of zero vectors.

After passing through a DSC and removing the first K_G zero vectors, the kth received signal vector $\mathbf{y}_k \in \mathbb{C}^{N_R\times 1}$ can be expressed as

[1] This GSM symbol formulation corresponds to the multiple active-SM symbol formulation in [9].

$$\mathbf{y}_k = \sum_{l=0}^{L_c-1} \mathbf{H}_{k,l}\mathbf{s}_{k-l} + \mathbf{w}_k, \quad k = 0, 1, \cdots, K + L_c - 2, \tag{3}$$

where $\mathbf{H}_{k,l}$ is the MIMO DSC corresponding to the lth channel tap at the kth time interval, as given by

$$\mathbf{H}_{k,l} = \begin{bmatrix} h_{k,l}^{0,0} & h_{k,l}^{1,0} & \cdots & h_{k,l}^{N_T-1,0} \\ h_{k,l}^{0,1} & h_{k,l}^{1,1} & \cdots & h_{k,l}^{N_T-1,1} \\ \vdots & \vdots & \ddots & \vdots \\ h_{k,l}^{0,N_R-1} & h_{k,l}^{1,N_R-1} & \cdots & h_{k,l}^{N_T-1,N_R-1} \end{bmatrix} \in \mathbb{C}^{N_R \times N_T} \tag{4}$$

with $h_{k,l}^{m,n}$ indicating the DSC coefficient between the mth transmit and nth receive antennas. Moreover, L_c is the number of channel taps, $\mathbf{w}_k \in \mathbb{C}^{N_R \times 1}$ denotes the complex additive white Gaussian noise vector with zero mean and covariance matrix $\sigma^2\mathbf{I}_{N_R}$, and $\mathbf{I}_N \in \mathbb{C}^{N \times N}$ is an identity matrix.

2.1. BEM representation of channel

BEM gives the most accurate representation of a DSC by modeling each channel tap as the linear superposition of basis functions [27]. Specifically, a DSC can be represented using BEM as [31]

$$h_{k,l}^{m,n} = \sum_{q=0}^{Q-1} b_{k,q} c_{l,q}^{m,n} = \mathbf{b}_k^T \mathbf{c}_l^{m,n}, \tag{5}$$

where $b_{k,q}$ is the qth basis function at the kth time interval, $c_{l,q}^{m,n}$ is the qth basis coefficient for the lth channel tap between the mth transmit and nth receive antennas, and Q is the number of basis coefficients. Besides, $\mathbf{b}_k = [b_{k,0}, b_{k,1}, \cdots, b_{k,Q-1}]^T$ and $\mathbf{c}_l^{m,n} = [c_{l,0}^{m,n}, c_{l,1}^{m,n}, \cdots, c_{l,Q-1}^{m,n}]^T$. Note that (5) originates from the physical representation of the mobile radio channel given by

$$h_{k,l}^{m,n} = \sum_{q=0}^{Q-1} a_{l,q}^{m,n} e^{j\frac{2\pi v}{\lambda}\cos(\frac{2\pi q}{Q})k}, \tag{6}$$

where Q and $a_{l,q}^{m,n}$ denote the number of paths and the complex (random) amplitude of the qth path, while v and λ are the speed of the propagating waves and the wavelength at the carrier frequency, respectively.

Then, we can write (4) as

$$\mathbf{H}_{k,l} = \mathbf{B}_k \mathbf{C}_l \tag{7}$$

where

$$\mathbf{B}_k = \begin{bmatrix} \mathbf{b}_k^T & \mathbf{0}_{1\times Q} & \mathbf{0}_{1\times Q} & \cdots & \mathbf{0}_{1\times Q} \\ \mathbf{0}_{1\times Q} & \mathbf{b}_k^T & \mathbf{0}_{1\times Q} & \cdots & \mathbf{0}_{1\times Q} \\ \vdots & \vdots & \ddots & & \vdots \\ \mathbf{0}_{1\times Q} & \mathbf{0}_{1\times Q} & \cdots & \mathbf{0}_{1\times Q} & \mathbf{b}_k^T \end{bmatrix} \in \mathbb{C}^{N_R \times N_R Q}, \tag{8}$$

and

$$\mathbf{C}_l = \begin{bmatrix} \mathbf{c}_l^{0,0} & \mathbf{c}_l^{1,0} & \cdots & \mathbf{c}_l^{N_T-1,0} \\ \mathbf{c}_l^{0,1} & \mathbf{c}_l^{1,1} & \cdots & \mathbf{c}_l^{N_T-1,1} \\ \vdots & \vdots & \ddots & \vdots \\ \mathbf{c}_l^{0,N_R-1} & \mathbf{c}_l^{1,N_R-1} & \cdots & \mathbf{c}_l^{N_T-1,N_R-1} \end{bmatrix} \in \mathbb{C}^{N_R Q \times N_T}. \tag{9}$$

Considering (5), BEM enables us to represent a time-varying channel in a separable form, as a product of basis functions $\mathbf{b}_k$ that vary over time but are known and basis coefficients $\mathbf{c}_l^{m,n}$ that do not change with time but are unknown. Several types of basis functions have been presented in the literature for this purpose, namely, the complex-exponential BEM (CE-BEM) [32], generalized complex-exponential BEM (GCE-BEM) [33], polynomial BEM (P-BEM) [34], and discrete Karhunen-loeve BEM (DKL-BEM) [35]. The DKL-BEM is known to provide the optimal channel representation in terms of mean square error (MSE). However, it requires the second order statistics of the channel, and is not robust to changes in channel statistics that occurs in practical situations. To overcome this shortcoming of the DKL-BEM, the CE-BEM, which does not require the knowledge of channel statistics, was presented in [32]. However, CE-BEM suffers from phase and amplitude errors due to the Gibbs phenomenon and spectral leakage [36]. The GCE-BEM is an improved version of the CE-BEM that is based on the use of complex exponentials more closely spaced in the frequency domain [37]. Alternatively, the P-BEM models temporal channel variations using linear combinations of polynomial terms [34], but its representation accuracy is sensitive to the Doppler spread. The interested reader is referred to [37] and the references therein for further details about different types of BEM.

In this paper, without loss of generality, we consider the GCE-BEM. In this model, the basis functions can be represented as

$$b_{k,q} = e^{j\frac{2\pi k}{\lambda K}(q-\frac{Q}{2})}, \quad k = 0, 1, \cdots, K + L_c - 2, \quad q = 0, 1, \cdots, Q - 1, \tag{10}$$

where $\lambda > 1$ is a design parameter. Having chosen the basis functions $b_{k,q}$ as per (10), it is possible to precisely construct the vectors $\mathbf{b}_k = [b_{k,0}, b_{k,1}, \cdots, b_{k,Q-1}]^T$ and matrices $\mathbf{B}_k$ in (8). Thus, in light of (7), it follows that to obtain $\mathbf{H}_{k,l}$, we only need to estimate $\mathbf{C}_l$. It is worth mentioning that the number of the basis coefficients Q is a small integer satisfying the condition $2f_D KT_s + 1 \le Q \ll K$ where f_D and T_s denote the maximum Doppler frequency and sampling time, respectively, [38–40]. In practice, the time-bandwidth product $f_D KT_s$ is relatively small, and typical values of Q are 2 to 3 [38].

Several methods have been proposed for the estimation of the basis coefficient matrix $\mathbf{C}_l$ in the literature. These methods usually either employ pilot symbols interlaced between data symbols, or use blocks of pilot symbols in between blocks of data symbols [41,42]. For instance, considering the second scenario, $\mathbf{C}_l$ is estimated using a block of pilots and, assuming that it does not change rapidly over time, it is used for representation of the time-varying channel over several subsequent data blocks. The least-squares method [43] and the Kalman filtering approach [40] are often used for the estimation of $\mathbf{C}_l$. It is worth mentioning that slight variations of $\mathbf{C}_l$ from the pilot block to the data blocks can also be predicted using interpolation [41,42]. The interested reader is referred to [41–46] and the references therein for further details in this regard.

Now, (7) enables us to express the kth received signal vector in terms of BEM as

$$\mathbf{y}_k = \mathbf{B}_k \sum_{l=0}^{L_c-1} \mathbf{C}_l \mathbf{s}_{k-l} + \mathbf{w}_k, \tag{11}$$

which shows that, disregarding the noise, the received signal is the product of $\mathbf{B}_k$ and the convolution $\sum_{l=0}^{L_c-1} \mathbf{C}_l \mathbf{s}_{k-l}$. Finally, the assembled received signal vectors $\mathbf{y} = [\mathbf{y}_0^T, \mathbf{y}_1^T, \cdots, \mathbf{y}_{K'}^T]^T$ can be shown as in (12) using BEM, where $K' = K + L_c - 2$ and $\mathbf{0}_{N_R \times N_T} \in \mathbb{R}^{N_R \times N_T}$ is an all zero matrix.

$$\underbrace{\begin{bmatrix}\mathbf{y}_0\\ \mathbf{y}_1\\ \vdots\\ \mathbf{y}_{K'}\end{bmatrix}}_{\mathbf{y}} = \underbrace{\begin{bmatrix} \mathbf{B}_0\mathbf{C}_0 & \mathbf{0}_{N_R\times N_T} & \cdots & \mathbf{0}_{N_R\times N_T} & \mathbf{0}_{N_R\times N_T} & \cdots & \mathbf{0}_{N_R\times N_T}\\ \mathbf{B}_1\mathbf{C}_1 & \mathbf{B}_1\mathbf{C}_0 & \cdots & \mathbf{0}_{N_R\times N_T} & \mathbf{0}_{N_R\times N_T} & \cdots & \mathbf{0}_{N_R\times N_T}\\ \vdots & \ddots & \vdots & \vdots & & & \\ \mathbf{B}_{L_c-1}\mathbf{C}_{L_c-1} & \mathbf{B}_{L_c-1}\mathbf{C}_{L_c-2} & \cdots & \mathbf{0}_{N_R\times N_T} & \mathbf{0}_{N_R\times N_T} & \cdots & \mathbf{0}_{N_R\times N_T}\\ \mathbf{0}_{N_R\times N_T} & \mathbf{B}_{L_c}\mathbf{C}_{L_c-1} & \cdots & \mathbf{B}_{L_c}\mathbf{C}_0 & \mathbf{0}_{N_R\times N_T} & \cdots & \mathbf{0}_{N_R\times N_T}\\ \vdots & & & \ddots & & & \vdots\\ \mathbf{0}_{N_R\times N_T} & \cdots & & \mathbf{B}_{K-1}\mathbf{C}_{L_c-1} & \cdots & \mathbf{B}_{K-1}\mathbf{C}_1 & \mathbf{B}_{K-1}\mathbf{C}_0\\ \mathbf{0}_{N_R\times N_T} & \cdots & & \vdots & \ddots & \vdots & \vdots\\ \mathbf{0}_{N_R\times N_T} & \cdots & & \mathbf{0}_{N_R\times N_T} & \cdots & \mathbf{B}_{K'-1}\mathbf{C}_{L_c-1} & \mathbf{B}_{K'-1}\mathbf{C}_{L_c-2}\\ \mathbf{0}_{N_R\times N_T} & \cdots & & \mathbf{0}_{N_R\times N_T} & \cdots & \mathbf{0}_{N_R\times N_T} & \mathbf{B}_{K'}\mathbf{C}_{L_c-1}\end{bmatrix}}_{\mathbf{G}} \times \underbrace{\begin{bmatrix}\mathbf{s}_0\\ \mathbf{s}_1\\ \vdots\\ \mathbf{s}_{K-1}\end{bmatrix}}_{\mathbf{s}} + \underbrace{\begin{bmatrix}\mathbf{w}_0\\ \mathbf{w}_1\\ \vdots\\ \mathbf{w}_{K'}\end{bmatrix}}_{\mathbf{w}} \tag{12}$$

3. Proposed methods based on maximum likelihood and partial interference cancellation

We first present a BML detection method which provides the processing framework for our proposed methods. Since the BML method is computationally inefficient, we then propose the BPIC and BPIC-SIC methods, which target the elimination of the interference between the GSM symbols within a block, to reduce the computational complexity.

3.1. BML method

Considering (12), the BML detection can be performed as

$$\hat{\mathbf{s}} = \arg\min_{\tilde{\mathbf{s}}\in\mathcal{S}} \|\mathbf{y} - \mathbf{G}\tilde{\mathbf{s}}\|^2, \tag{13}$$

where the trial values of the signal vectors and the detected signal vectors corresponding to $\mathbf{s}$ are shown by $\tilde{\mathbf{s}}$ and $\hat{\mathbf{s}}$, respectively. Besides, $\mathcal{S}$ denotes the set of all valid transmit vectors for a block of GSM symbols, whose number of elements is μ^K where $\mu = 2^{\log_2\zeta + \left\lfloor \log_2\binom{N_T}{N_a}\right\rfloor}$. Note that the detection of $\tilde{\mathbf{s}}$ in (13) takes into account the special structure of the GSM symbols $\mathbf{s}_k$, $k = 0, \cdots, K-1$, comprising the composite vector $\mathbf{s}$ in (12). This is reflected in the construction and use of the search space $\mathcal{S}$, which is equivalent for each GSM symbol $\mathbf{s}_k$ to detecting which subset of N_a antennas are active within the available N_T transmit antennas, and which symbols are transmitted through the active antennas.

Since the BML method requires an exhaustive search over all valid signal vectors, it is of a very high computational complexity and becomes impractical for even small values of the system parameters. Hence, in the next subsections, we will introduce methods that have significantly lower complexity yet can achieve satisfactory performances.

3.2. BPIC method

PIC was proposed in [47] for group decoding of space-time block codes, and was used in [17] for SC-SM signal detection in slow fading frequency selective channels where the channel remains constant within a block of SM symbol. Here, we propose a new method for SC-GSM signal detection in a DSC where, using BEM, the PIC method is tailored to cope with time-variations of a DSC.

Considering (12), we can equivalently write the received signal as

$$\mathbf{y} = \sum_{k=0}^{K-1} \bar{\mathbf{B}}\mathbf{C}_{\mathcal{I}_k}\mathbf{s}_k + \mathbf{w}, \tag{14}$$

where

$$\bar{\mathbf{B}} = \begin{bmatrix} \mathbf{B}_0 & \mathbf{0}_{N_R\times N_RQ} & \cdots & \mathbf{0}_{N_R\times N_RQ}\\ \mathbf{0}_{N_R\times N_RQ} & \mathbf{B}_1 & \cdots & \mathbf{0}_{N_R\times N_RQ}\\ \vdots & \vdots & \ddots & \vdots\\ \mathbf{0}_{N_R\times N_RQ} & \cdots & \mathbf{0}_{N_R\times N_RQ} & \mathbf{B}_{K'}\end{bmatrix} \in \mathbb{C}^{N_R(K+L_c-1)\times N_RQ(K+L_c-1)}, \tag{15}$$

$\mathbf{C}_{\mathcal{I}_k}$ is the matrix whose columns are columns of $\mathbf{C}$ that are indexed by the elements of $\mathcal{I}_k$, $\mathbf{C}\in\mathbb{C}^{N_RQ(K+L_c-1)\times N_TK}$ denotes a block Toeplitz matrix with the first column $[\mathbf{C}_0^T, \mathbf{C}_1^T, \cdots, \mathbf{C}_{L_c-1}^T, \mathbf{0}_{N_T\times N_RQ}, \cdots, \mathbf{0}_{N_T\times N_RQ}]^T$, and $\mathcal{I}_k = \{N_Tk, N_Tk+1, \cdots, N_Tk+N_T-1\}$. Next, for $m = 0, 1, \cdots, K-1$, we project $\mathbf{y}$ onto the orthogonal complement space of

$$\mathbf{T}_{\mathcal{I}_m} = \left[\bar{\mathbf{B}}\mathbf{C}_{\mathcal{I}_0}, \cdots, \bar{\mathbf{B}}\mathbf{C}_{\mathcal{I}_{m-1}}, \bar{\mathbf{B}}\mathbf{C}_{\mathcal{I}_{m+1}}, \cdots, \bar{\mathbf{B}}\mathbf{C}_{\mathcal{I}_{K-1}}\right], \tag{16}$$

using the orthogonal projection operator

$$\mathbf{\Pi}_{\mathcal{I}_m}^{\perp} = \mathbf{I}_{N_R(K'+1)} - \mathbf{T}_{\mathcal{I}_m}\left(\mathbf{T}_{\mathcal{I}_m}^H\mathbf{T}_{\mathcal{I}_m}\right)^{-1}\mathbf{T}_{\mathcal{I}_m}^H, \tag{17}$$

where $(\cdot)^H$ denotes the Hermitian operation. Thus, we have

$$\mathbf{u}_m = \mathbf{\Pi}_{\mathcal{I}_m}^{\perp}\mathbf{y} = \mathbf{\Pi}_{\mathcal{I}_m}^{\perp}\sum_{k=0}^{K-1}\bar{\mathbf{B}}\mathbf{C}_{\mathcal{I}_k}\mathbf{s}_k + \mathbf{\Pi}_{\mathcal{I}_m}^{\perp}\mathbf{w}_k = \mathbf{\Pi}_{\mathcal{I}_m}^{\perp}\bar{\mathbf{B}}\mathbf{C}_{\mathcal{I}_m}\mathbf{s}_m + \mathbf{\Pi}_{\mathcal{I}_m}^{\perp}\mathbf{w}_k, \tag{18}$$

where the last equality results from $\mathbf{\Pi}_{\mathcal{I}_m}^{\perp}\bar{\mathbf{B}}\mathbf{C}_{\mathcal{I}_k} = \mathbf{0}_{N_R(K'+1)\times N_T}$, $k\neq m$. As shown in (18), the signal term in $\mathbf{u}_m$ contains only $\mathbf{s}_m$, and the interferences from other signals $\mathbf{s}_k, k\neq m$ are canceled. Now, the signal at the mth time interval can be detected as

$$\hat{\mathbf{s}}_m = \arg\min_{\tilde{\mathbf{s}}_m\in\mathcal{S}_m}\left\|\mathbf{u}_m - \mathbf{\Pi}_{\mathcal{I}_m}^{\perp}\bar{\mathbf{B}}\mathbf{C}_{\mathcal{I}_m}\tilde{\mathbf{s}}_m\right\|^2, \tag{19}$$

where $\tilde{\mathbf{s}}_m$ is the trial value of $\mathbf{s}_m$, and $\mathcal{S}_m$ denotes the set including all valid transmit vectors for a GSM symbol whose number of elements is μ. This method is summarized in Algorithm 1.

Algorithm 1 BPIC Method.

1: Inputs: $\mathbf{y}$, $\bar{\mathbf{B}}$, $\mathcal{I}_m$, and $\mathbf{C}$.
2: **for** m from 0 to $K-1$ **do**
3: Generate the projection matrix for the mth signal vector

$$\mathbf{\Pi}_{\mathcal{I}_m}^{\perp} = \mathbf{I}_{N_R(K'+1)} - \mathbf{T}_{\mathcal{I}_m}\left(\mathbf{T}_{\mathcal{I}_m}^H\mathbf{T}_{\mathcal{I}_m}\right)^{-1}\mathbf{T}_{\mathcal{I}_m}^H \tag{20}$$

where

$$\mathbf{T}_{\mathcal{I}_m} = \left[\bar{\mathbf{B}}\mathbf{C}_{\mathcal{I}_0}, \cdots, \bar{\mathbf{B}}\mathbf{C}_{\mathcal{I}_{m-1}}, \bar{\mathbf{B}}\mathbf{C}_{\mathcal{I}_{m+1}}, \cdots, \bar{\mathbf{B}}\mathbf{C}_{\mathcal{I}_{K-1}}\right]. \tag{21}$$

4: Project $\mathbf{y}$ onto the orthogonal complement spaceof $\mathbf{T}_{\mathcal{I}_m}$ as

$$\mathbf{u}_m = \mathbf{\Pi}_{\mathcal{I}_m}^{\perp}\mathbf{y} \tag{22}$$

5: Detect the mth transmitted vector as

$$\hat{\mathbf{s}}_m = \arg\min_{\tilde{\mathbf{s}}_m\in\mathcal{S}_m}\left\|\mathbf{u}_m - \mathbf{\Pi}_{\mathcal{I}_m}^{\perp}\bar{\mathbf{B}}\mathbf{C}_{\mathcal{I}_m}\tilde{\mathbf{s}}_m\right\|^2. \tag{23}$$

6: **end for**

It is worth noting that the detection of $\mathbf{s}_m$ in (23) is tantamount to detecting the special structure of the transmitted vector $\mathbf{s}_k$, i.e., detecting which antennas are active and which signals are

transmitted through the active antennas. To elaborate on this issue, we express (1) as $\mathbf{s}_k = \mathbf{F}_k \dot{\mathbf{s}}_k$ where $\dot{\mathbf{s}}_k = [s_{k,0}, s_{k,1}, \cdots, s_{k,N_a-1}]^T$ and $\mathbf{F}_k \in \mathbb{C}^{N_T \times N_a}$ such that $\mathbf{F}_k \in \mathcal{F} = \{F_0, F_1, \cdots, F_{N_T-1}\}$. Besides, the vector F_m denotes the mth column of a $N_T \times N_T$ identity matrix. Hence, for detecting $\mathbf{s}_k$, it suffices to detect $\dot{\mathbf{s}}_k$ and the position of nonzero elements of $\mathbf{F}_k$, which can be performed using an exhaustive search. Other simplified algorithms such as those in [48] and [49] can also be applied.

3.3. BPIC-SIC method

The idea behind the SIC is the elimination of already detected signals from the received signal with the goal of reducing the interferences [47] and improving the detection performance while limiting the complexity. This method is also used in [47] and [17] for group decoding of space-time block codes and SC-SM signal detection in slow fading frequency selective channels, respectively. Here, we propose the BPIC-SIC method for detection of SC-GSM signals in a DSC.

The new method starts with the use of the BPIC method for the detection of the zeroth received signal vector, i.e. $\mathbf{s}_0$. Subsequently, for the remaining $K-1$ signal vectors $\mathbf{s}_m$, $m = 1, \cdots, K-1$, two steps are taken. First, the interference term caused by the already detected signals is removed, and second, projection onto the orthogonal complement space of the channel corresponding to the remaining undetected signals is carried out. This method is described in Algorithm 2.

Algorithm 2 BPIC-SIC Method.

1: Inputs: $\mathbf{y}$, $\bar{\mathbf{B}}$, $\mathcal{I}_m$, and $\mathbf{C}$.
2: Detect the 0th transmit signal vector $\mathbf{s}_0$ using the BPIC approach, and put $\mathbf{y}^{(m)} = \mathbf{y}$.
3: **for** m from 0 to $K-2$ **do**
4: Remove the interference caused by the already detected signals

$$\mathbf{y}^{(m+1)} = \mathbf{y}^{(m)} - \bar{\mathbf{B}}\mathbf{C}_{\mathcal{I}_m}\mathbf{s}_m \tag{24}$$

5: Generate the projection matrix

$$\mathbf{\Pi}^{\perp}_{\mathcal{I}_{m+1}} = \mathbf{I}_{N_R(K'+1)} - \mathbf{T}_{\mathcal{I}_{m+1}}\left(\mathbf{T}^H_{\mathcal{I}_{m+1}}\mathbf{T}_{\mathcal{I}_{m+1}}\right)^{-1}\mathbf{T}^H_{\mathcal{I}_{m+1}} \tag{25}$$

where

$$\mathbf{T}_{\mathcal{I}_{m+1}} = \left[\bar{\mathbf{B}}\mathbf{C}_{\mathcal{I}_{m+2}}, \bar{\mathbf{B}}\mathbf{C}_{\mathcal{I}_{m+3}}, \cdots, \bar{\mathbf{B}}\mathbf{C}_{\mathcal{I}_{K-1}}\right] \tag{26}$$

6: Project $\mathbf{y}^{(m+1)}$ onto the orthogonal complement space of $\mathbf{T}_{\mathcal{I}_{m+1}}$ as

$$\mathbf{u}_{m+1} = \mathbf{\Pi}^{\perp}_{\mathcal{I}_{m+1}}\mathbf{y}^{(m+1)} \tag{27}$$

7: Detect the $(m+1)$th transmitted vector as

$$\hat{\mathbf{s}}_{m+1} = \arg\min_{\tilde{\mathbf{s}}_{m+1}\in\mathcal{S}_m} \left\|\mathbf{u}_{m+1} - \mathbf{\Pi}^{\perp}_{\mathcal{I}_{m+1}}\bar{\mathbf{B}}\mathbf{C}_{\mathcal{I}_{m+1}}\tilde{\mathbf{s}}_{m+1}\right\|^2. \tag{28}$$

8: **end for**

It is worth mentioning that the BPIC and BPIC-SIC methods should meet the condition $(K+L_c-1)N_R \geq (K-1)N_T$ for achieving satisfactory performance. This condition is necessary to ensure that $\mathbf{T}_{\mathcal{I}_m}$, $m = 0, \cdots, K-1$ is a column full-rank matrix. Otherwise, $\mathbf{T}_{\mathcal{I}_m}$ becomes rank deficient which results in inaccurate detection [19]. We note that this condition is dependent on the number of channel taps L_c, and can be satisfied even when $N_R < N_T$ if L_c is sufficiently large. In effect, this is due to the multipath (delay) diversity along with the use of zero-padding in the transmission process. However, for the practical case where the number of receive antennas is no less than the number of transmit antennas, i.e., $N_R \geq N_T$, the condition is always satisfied independent of L_c.

In addition to not satisfying the above condition, there can be other scenarios in which the matrix $\mathbf{T}_{\mathcal{I}_m}$ becomes rank deficient, for instance, when the columns of $\mathbf{T}_{\mathcal{I}_m}$, due to the choices of BEM functions and their corresponding coefficients, are linearly dependent. Moreover, as shown in (20) and (25), the BPIC and BPIC-SIC methods call for the calculation of a matrix inverse of for each $m = 0, \cdots, K-1$, which imposes a high computational burden. In the next section, we will propose methods whose performance does not depend on the condition $(K+L_c-1)N_R \geq (K-1)N_T$, and do not require matrix inversion.

4. Proposed tree search-based methods

In this section, we present new methods based on tree search with the goal of further reducing the complexity and overcoming the limitations of the BPIC and BPIC-SIC methods for SC-GSM signal detection in a DSC. The first two methods use the minimum values of a cost function to prune the search tree, whereas the third one exploits sphere decoding for this purpose.

4.1. BTS method

The proposed BTS method employs the tree search-based method in [19]. In particular, the latter method developed for slow fading channels is modified to take the time-variations of a DSC into account. In the proposed tree search method, the tree is composed of nodes, branches, and a metric assigned to each branch. Nodes with depth k in the tree ($k = 0, 1, \cdots, K-1$) represent different values of $\tilde{\mathbf{s}}_k$, and are connected to all nodes with depth $k+1$. The metric corresponding to each branch is the measure of correctness of the branch and is designed based on the least squares cost function. Lastly, the criterion for pruning the tree is based on the minimum values of the cost function. Fig. 1 depicts the structure of the considered tree where $\tilde{\mathbf{s}}_{m,n}$ denotes the nth trial value of the mth received vector. In what follows, we explain the proposed method for designing the metric and pruning the tree in detail.

The zeroth received signal vector can be written as

$$\mathbf{y}_0 = \mathbf{B}_0\mathbf{C}_0\mathbf{s}_0 + \mathbf{w}_0 \tag{29}$$

which results in the least squares cost function

$$\Lambda(\tilde{\mathbf{s}}_0) = \left\|\mathbf{y}_0 - \mathbf{B}_0\mathbf{C}_0\tilde{\mathbf{s}}_0\right\|^2. \tag{30}$$

We calculate $\Lambda(\tilde{\mathbf{s}}_0)$ for all μ values of $\tilde{\mathbf{s}}_0$ and arrange $\Lambda(\tilde{\mathbf{s}}_0)$ for different values of $\tilde{\mathbf{s}}_0$ in ascending order of magnitude. We then put the first η values of $\Lambda(\tilde{\mathbf{s}}_0)$ and their corresponding $\tilde{\mathbf{s}}_0$ in the vectors $\mathbf{\Gamma}_0 = [\Lambda(\mathbf{a}_{0,0}), \Lambda(\mathbf{a}_{0,1}), \cdots, \Lambda(\mathbf{a}_{0,\eta-1})]$ and $\mathbf{\Phi}_0 = [\mathbf{a}_{0,0}, \mathbf{a}_{0,1}, \cdots, \mathbf{a}_{0,\eta-1}]$, respectively, where $\mathbf{a}_{0,m}$ is the mth selected $\tilde{\mathbf{s}}_0$ at the zero-th step and η is a chosen positive integer.

Next, for the zeroth and first received vectors, we have

$$\begin{bmatrix}\mathbf{y}_0\\ \mathbf{y}_1\end{bmatrix} = \begin{bmatrix}\mathbf{B}_0\mathbf{C}_0 & \mathbf{0}_{N_R\times N_T}\\ \mathbf{B}_1\mathbf{C}_1 & \mathbf{B}_1\mathbf{C}_0\end{bmatrix}\begin{bmatrix}\mathbf{s}_0\\ \mathbf{s}_1\end{bmatrix} + \begin{bmatrix}\mathbf{w}_0\\ \mathbf{w}_1\end{bmatrix} \tag{31}$$

for which the cost function can be written as

$$\begin{aligned}\Lambda(\tilde{\mathbf{s}}_0, \tilde{\mathbf{s}}_1) &= \left\|\begin{bmatrix}\mathbf{y}_0\\ \mathbf{y}_1\end{bmatrix} - \begin{bmatrix}\mathbf{B}_0\mathbf{C}_0 & \mathbf{0}_{N_R\times N_T}\\ \mathbf{B}_1\mathbf{C}_1 & \mathbf{B}_1\mathbf{C}_0\end{bmatrix}\begin{bmatrix}\tilde{\mathbf{s}}_0\\ \tilde{\mathbf{s}}_1\end{bmatrix}\right\|^2\\ &= \Lambda(\tilde{\mathbf{s}}_0) + \left\|\mathbf{y}_1 - \begin{bmatrix}\mathbf{B}_1\mathbf{C}_1 & \mathbf{B}_1\mathbf{C}_0\end{bmatrix}\begin{bmatrix}\tilde{\mathbf{s}}_0\\ \tilde{\mathbf{s}}_1\end{bmatrix}\right\|^2.\end{aligned} \tag{32}$$

Now, we respectively replace $\tilde{\mathbf{s}}_0$ and $\Lambda(\tilde{\mathbf{s}}_0)$ with the selected values of $\tilde{\mathbf{s}}_0$ and $\Lambda(\tilde{\mathbf{s}}_0)$ in the previous step i.e., $\mathbf{a}_{0,m}$ and $\Lambda(\mathbf{a}_{0,m})$, $m = 0, 1, \cdots, \eta-1$. After computing all $\mu\eta$ values of $\Lambda(\mathbf{a}_{0,m}, \tilde{\mathbf{s}}_1)$ for different values of $\mathbf{a}_{0,m}$ and $\tilde{\mathbf{s}}_1$, we again arrange them in ascending order of magnitude, and choose the first η elements as $\mathbf{\Gamma}_1 = [\Lambda(\mathbf{a}_{1,0}), \Lambda(\mathbf{a}_{1,1}), \cdots, \Lambda(\mathbf{a}_{1,\eta-1})]$ where $\mathbf{a}_{1,l}$ is the lth value

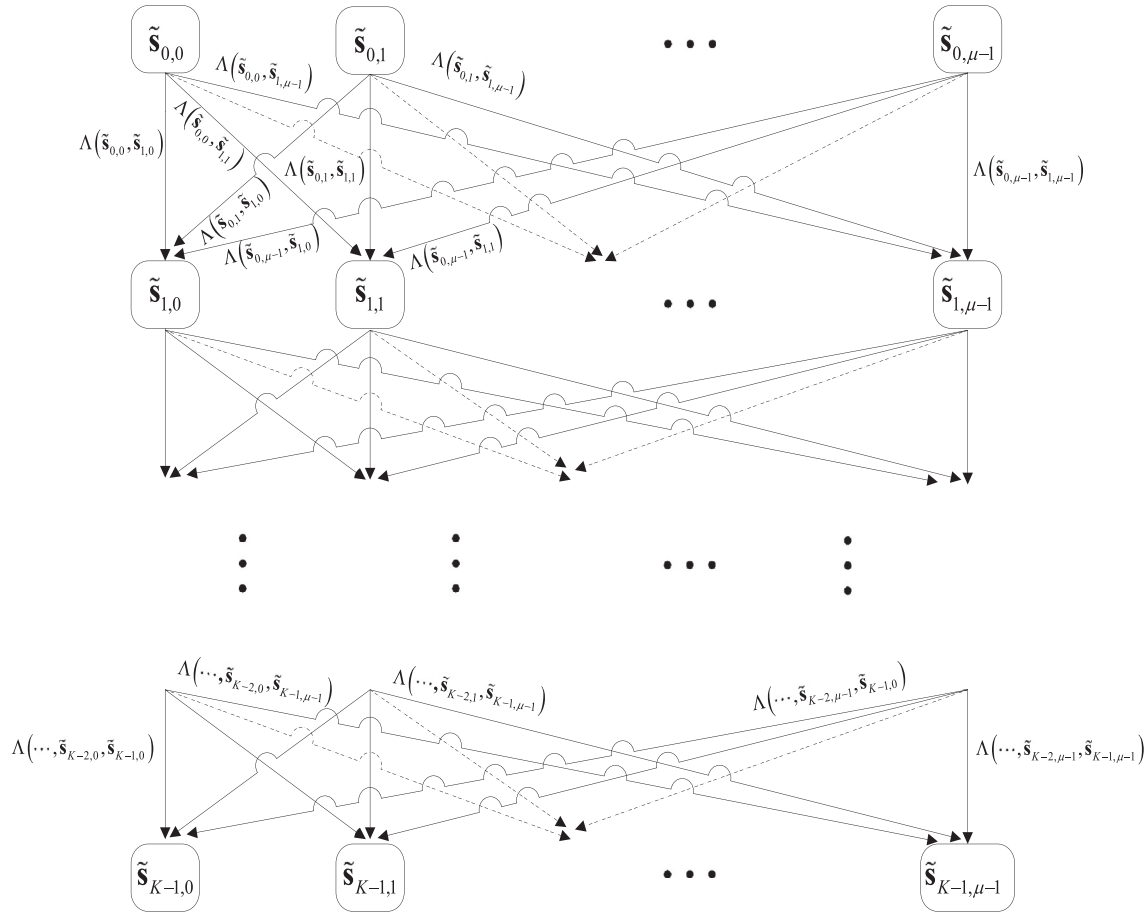

Fig. 1. Graphical model of the tree structure for the proposed tree-search algorithms.

of $[\mathbf{a}_{0,l}^T, \tilde{\mathbf{s}}_1^T]^T$ at this step (i.e. step 1) and we also obtain $\mathbf{\Phi}_1 = [\mathbf{a}_{1,0}, \mathbf{a}_{1,1}, \cdots, \mathbf{a}_{1,\eta-1}]$.

This procedure continues until the $(K-1)$th step at which $\mathbf{\Gamma}_{K-1} = [\Lambda(\mathbf{a}_{K-1,0}), \Lambda(\mathbf{a}_{K-1,1}), \cdots, \Lambda(\mathbf{a}_{K-1,\eta-1})]$ is calculated, and the corresponding

$$\mathbf{\Phi}_{K-1} = [\mathbf{a}_{K-1,0}, \mathbf{a}_{K-1,1}, \cdots, \mathbf{a}_{K-1,\eta-1}] \tag{33}$$

is obtained. Finally, considering (12) and the selected trial values $[\tilde{\mathbf{s}}_0^T, \tilde{\mathbf{s}}_1^T, \cdots, \tilde{\mathbf{s}}_{K-1}^T]^T$ as $\mathbf{a}_{K-1,m}$, $m = 0, 1, \cdots, \eta-1$ in (33), the signal vectors are detected as

$$\hat{\mathbf{s}} = \arg \min_{\mathbf{a}_{K-1,m} \in \mathbf{\Phi}_{K-1}} \|\mathbf{y} - \mathbf{G}\mathbf{a}_{K-1,m}\|^2. \tag{34}$$

This method is summarized in Algorithm 3, where $\eta_{initial}$ denotes the initial value of η. Note that $\eta_{initial} = 1$ as $\mathbf{a}_{k-1,m}$ is an empty set at the beginning of the algorithm. Afterwards, we should have $\eta > 1$. In general, the greater the values of η, the better the performance, but the higher the complexity, as explained in the next section (Fig. 12 and Table 1).

4.2. BRCTS method

To obtain the cost function in the BTS method, as indicated in (35), for each k, m, and $\tilde{\mathbf{s}}_k \in \mathcal{S}_k$, the matrix $\mathbf{G}_k \in \mathbb{C}^{N_R(k+1)\times N_T(k+1)}$ should be multiplied by $[\tilde{\mathbf{s}}_0, \cdots, \tilde{\mathbf{s}}_k]^T$. The complexity of the BTS method can be considerably reduced by taking into account the fact that the channel has L_c taps, and therefore, the received signal is the superposition of at most L_c transmitted signals. In other words, as can be seen in (12), each row of $\mathbf{G}$ and consequently $\mathbf{G}_k$ has at most L_c nonzero $N_R \times N_T$ blocks. Here, to reduce the complexity, we propose to replace $\mathbf{G}_k$ with a matrix that contains only

Algorithm 3 BTS Method.

1: Inputs: $\mathbf{y}$, $\mathbf{B}_k$, $\mathbf{C}_l$, $\mathbf{a}_{-1,0} = [\ ]$, $\Lambda(\mathbf{a}_{-1,0}) = 0$, $\eta_{initial} = 1$.
2: **for** k from 0 to $K-1$ **do**
3: **for** m from 0 to $\eta - 1$ **do**
4: **for** $\tilde{\mathbf{s}}_k \in \mathcal{S}_k$ **do**
5: Calculate the cost function

$$\Lambda(\mathbf{a}_{k-1,m}, \tilde{\mathbf{s}}_k) = \Lambda(\mathbf{a}_{k-1,m}) + \left\| \mathbf{y}_k - \mathbf{G}_k \begin{bmatrix} \tilde{\mathbf{s}}_0 \\ \vdots \\ \tilde{\mathbf{s}}_k \end{bmatrix} \right\|^2 \tag{35}$$

where $\mathbf{G}_k$ is a matrix containing rows 0 to $N_R k$ and columns 0 to $N_T k$ of $\mathbf{G}$.

6: **end for**
7: **end for**
8: Arrange values of $\Lambda(\mathbf{a}_{k-1,m}, \tilde{\mathbf{s}}_k)$ in ascending order of magnitude
9: Select the first η values of the arranged elements and the corresponding $\mathbf{a}_{k,l} = [\mathbf{a}_{k-1,l}^T, \tilde{\mathbf{s}}_k^T]^T$ as

$$\mathbf{\Gamma}_k = [\Lambda(\mathbf{a}_{k,0}), \Lambda(\mathbf{a}_{k,1}), \cdots, \Lambda(\mathbf{a}_{k,\eta-1})] \tag{36}$$

$$\mathbf{\Phi}_k = [\mathbf{a}_{k,0}, \mathbf{a}_{k,1}, \cdots, \mathbf{a}_{k,\eta-1}] \tag{37}$$

10: **end for**
11: Detect the signal vectors as

$$\hat{\mathbf{s}} = \arg \min_{\mathbf{a}_{K-1,m} \in \mathbf{\Phi}_{K-1}} \left\| \mathbf{y} - \mathbf{G}\mathbf{a}_{K-1,m} \right\|^2. \tag{38}$$

nonzero elements of $\mathbf{G}_k$, and also modify $[\mathbf{s}_0, \cdots, \mathbf{s}_k]^T$ accordingly. This method is presented as Algorithm 4.

Algorithm 4 BRCTS Method.

Inputs: $\mathbf{y}$, $\mathbf{B}_k$, $\mathbf{C}_l$, $\mathbf{a}_{-1,0} = [\ ]$, $\Lambda(\mathbf{a}_{-1,0}) = 0$, $\eta_{initial} = 1$.
for k from 0 to $K-1$ **do**
  for m from 0 to $\eta - 1$ **do**
    for $\tilde{\mathbf{s}}_k \in \mathcal{S}_k$ **do**
      Calculate the cost function

$$\Lambda(\mathbf{a}_{k-1,m}, \tilde{\mathbf{s}}_k) = \Lambda(\mathbf{a}_{k-1,m}) + \left\| \mathbf{y}_k - \begin{bmatrix} \mathbf{B}_k\mathbf{C}_u & \cdots & \mathbf{B}_k\mathbf{C}_0 \end{bmatrix} \begin{bmatrix} \tilde{\mathbf{s}}_{k-u} \\ \vdots \\ \tilde{\mathbf{s}}_k \end{bmatrix} \right\|^2 \tag{39}$$

where

$$u = \begin{cases} L_c - 1 & \text{if } k \geq L_c - 1 \\ k & \text{otherwise.} \end{cases} \tag{40}$$

    end for
  end for
  Arrange values of $\Lambda(\mathbf{a}_{k-1,m}, \tilde{\mathbf{s}}_k)$in ascending orderof magnitude
  Select the first η values of the ordered elements andthe corresponding $\mathbf{a}_{k,m} = [\mathbf{a}_{k-1,m}^T, \tilde{\mathbf{s}}_k^T]^T$ as

$$\mathbf{\Gamma}_k = [\Lambda(\mathbf{a}_{k,0}), \Lambda(\mathbf{a}_{k,1}), \cdots, \Lambda(\mathbf{a}_{k,\eta-1})] \tag{41}$$

$$\mathbf{\Phi}_k = \left[\mathbf{a}_{k,0}, \mathbf{a}_{k,1}, \cdots, \mathbf{a}_{k,\eta-1}\right] \tag{42}$$

end for
Detect the signal vectors as

$$\hat{\mathbf{s}} = \arg \min_{\mathbf{a}_{K-1,m} \in \mathbf{\Phi}_{K-1}} \left\| \mathbf{y} - \mathbf{G}\mathbf{a}_{K-1,m} \right\|^2. \tag{43}$$

4.3. BRCTS-SD method

The proposed BRCTS-SD method for signal detection in DSCs is based on the SM-Tx method in [50] developed for SM in slow fading frequency flat channels, and the LC-ESD-Tx method in [20] presented for SC-GSM in slow fading frequency selective channels. The proposed BRCTS-SD detector is also a tree-search based method similar to the proposed BTS and BRCTS detectors. The main distinction is that in the BRCTS-SD method we use the principle of sphere decoding [20,50,51] in order to reduce the search space by taking into account only the points that lie within a certain distance from the received signal [51].

The new method begins with the calculation of

$$\Lambda(\tilde{\mathbf{s}}_0) = \left\| \mathbf{y}_0 - \mathbf{B}_0\mathbf{C}_0\tilde{\mathbf{s}}_0 \right\|^2. \tag{44}$$

All $\tilde{\mathbf{s}}_0$ satisfying the condition $\Lambda(\tilde{\mathbf{s}}_0) < R^2$ are stored as $\mathbf{a}_{0,m}$, $m = 0, 1, \cdots, \eta_0 - 1$, where $R = \sqrt{\alpha N_R \sigma^2}$ is the radius, $\alpha > 0$ is a parameter that can be chosen flexibly based on antenna configuration [20,50], and η_0 is the number of vectors $\tilde{\mathbf{s}}_0$ satisfying the condition. Next,

$$\Lambda(\mathbf{a}_{0,m}, \tilde{\mathbf{s}}_1) = \left\| \mathbf{y}_1 - \begin{bmatrix} \mathbf{B}_1\mathbf{C}_1 & \mathbf{B}_1\mathbf{C}_0 \end{bmatrix} \begin{bmatrix} \mathbf{a}_{0,m} \\ \tilde{\mathbf{s}}_1 \end{bmatrix} \right\|^2 \tag{45}$$

is calculated for $\mathbf{a}_{0,m}$, $m = 0, 1, \cdots, \eta_0 - 1$ and all possible trial vectors $\tilde{\mathbf{s}}_1$. Those $\mathbf{a}_{0,m}$ and $\tilde{\mathbf{s}}_1$ vectors meeting the condition $\Lambda(\mathbf{a}_{0,m}, \tilde{\mathbf{s}}_1) < R^2 + \Lambda(\mathbf{a}_{0,m})$ are again selected and stored as $\mathbf{a}_{1,l} = [\mathbf{a}_{0,l}^T, \tilde{\mathbf{s}}_1^T]^T$. This process is continued until all $\mathbf{a}_{K-1,l}$, $l = 0, 1, \cdots, \eta_{K-1} - 1$ are found. Finally, (38) is utilized to detect the signal vectors.

There are cases where either too many vectors or no vectors at all satisfy the above condition. In the former case, a specified number of vectors, say η, that satisfy the condition and correspond to the least values of the cost function can be selected. In the latter case, η vectors from all valid vectors that correspond to the least values of the cost function can be selected. The BRCTS-SD method is presented in Algorithm 5, at the end of the paper.

Algorithm 5 BRCTS-SD Method.

Inputs: $\mathbf{y}$, $\mathbf{B}_k, \mathbf{C}_l$, $\mathbf{a}_{-1,0} \in \emptyset$, $\eta_{-1} = 1$, $\mathbf{\Phi}_k = [\ ]$, $\mathbf{\Gamma}_k \in \emptyset$.
for k from 0 to $K-1$ **do**
  $\eta_k = 0$
  for m from 0 to $\eta_{k-1} - 1$ **do**
    for $\tilde{\mathbf{s}}_k \in \mathcal{S}$ **do**
      Calculate the cost function as

$$\Lambda(\mathbf{a}_{k-1,m}, \tilde{\mathbf{s}}_k) = \left\| \mathbf{y}_k - \begin{bmatrix} \mathbf{B}_k\mathbf{C}_u & \cdots & \mathbf{B}_k\mathbf{C}_0 \end{bmatrix} \begin{bmatrix} \tilde{\mathbf{s}}_{k-u} \\ \vdots \\ \tilde{\mathbf{s}}_k \end{bmatrix} \right\|^2 \tag{46}$$

      where u is given in (40).
      if $\Lambda(\mathbf{a}_{k-1,m}, \tilde{\mathbf{s}}_k) < R^2 + \Lambda(\mathbf{a}_{k-1,m})$ **then**
        Save $\mathbf{a}_{k,m} = [\mathbf{a}_{k-1,m}^T, \tilde{\mathbf{s}}_k^T]^T$ and$\Lambda(\mathbf{a}_{k-1,m}, \tilde{\mathbf{s}}_k)$ as $\mathbf{\Phi}_k = [\mathbf{\Phi}_k, \mathbf{a}_{k,m}]$ and$\mathbf{\Gamma}_k = [\mathbf{\Gamma}_k, \Lambda(\mathbf{a}_{k-1,m}, \tilde{\mathbf{s}}_k)]$.
        $\eta_k = \eta_k + 1$.
      end if
    end for
  end for
  if $\eta_k > \eta$ **then**
    Arrange elements of $\mathbf{\Gamma}_k$ in ascending order of magnitude.
    Return the first η elements of the ordered $\mathbf{\Gamma}_k$ as$\mathbf{\Gamma}_k$ and the corresponding η columns of $\mathbf{\Phi}_k$ as $\mathbf{\Phi}_k$.
    Set $\eta_k = \eta$.
  else if $\eta_k = 0$ **then**
    Arrange values of $\Lambda(\mathbf{a}_{k-1,m}, \tilde{\mathbf{s}}_k)$in ascending order of magnitude.
    Return the first η ordered elements as $\mathbf{\Gamma}_k$ and the corresponding η vectors $\left[\mathbf{a}_{k-1,m}^T, \tilde{\mathbf{s}}_k^T\right]^T$ as $\mathbf{\Phi}_k$.
    Set $\eta_k = \eta$.
  end if
end for
Detect the signal vectors as

$$\hat{\mathbf{s}} = \arg \min_{\mathbf{a}_{K-1,m} \in \mathbf{\Phi}_{K-1}} \|\mathbf{y} - \mathbf{G}\mathbf{a}_{K-1,m}\|^2. \tag{47}$$

To conclude this section, it is worth mentioning that for each k, the proposed tree search methods selects η values of the trial vectors corresponding to the least values of the cost function. In this regard, the parameter η provides a means of robustness against poor decisions on the choice of $\mathbf{s}_k$, $k = 0, 1, \cdots, K-1$, and consequently can reduce error propagation. As η increases, for each k, more trial values of $\mathbf{s}_k$ are selected as candidates for the true value of $\mathbf{s}_k$. Hence, the detection of $\mathbf{s}_k$ becomes less reliant on specific choices of already selected candidates at lower depth i.e. $k' < k$. The performance improvement of the tree search methods with increasing η due to the above-mentioned reason is further validated by simulation results in Section V. Finally, we note that due to the zero-padding (see (2)), $\mathbf{s}_0$ in (29) is not affected by inter-block and inter-symbol interference, and it is therefore justified to use it as the anchor node in the tree search.

Table 1
Computational complexity of detection methods.

Method	Number of multiplications	Number of additions
PIC	$K\big((N_T(K-1))^3+2N_T^2N_RK'(K-1)^2+N_TN_R^2K'^2(K-1)+(N_RK')^2+\mu N_RK'N_T\big)$	$\big((N_T(K-1))^3+N_T^2(N_RK'-1)(K-1)^2+N_T(K-1)(N_T(K-1)-1)N_RK'+N_TN_R^2K'^2(K-1)-N_RK'+N_RK'(N_RK'-1)+\mu N_RK'(N_T-1)\big)$
PIC-SIC	$\sum_{k=1}^{K}\big((N_Tk)^3+2N_T^2N_RK'k^2+N_TN_R^2K'^2k+(N_RK')^2+\mu N_RK'N_T\big)$	$\sum_{k=1}^{K}\big((N_Tk)^3+N_T^2(N_RK'-1)k^2+N_Tk(N_Tk-1)N_RK'+(N_Tk-1)N_R^2K'^2+N_T-1+(N_RK')(N_RK'-1)+\mu N_RK'(N_T-1)\big)$
PIC-SIC-LaMP	$\sum_{k=1}^{K}\big((N_Tk)^3+2N_T^2N_RK'k^2+N_TN_R^2K'^2k+(N_RK')^2+N_{la}((3+\mu)N_RN_T-3N_T+2N_T^2)\big)$	$\sum_{k=1}^{K}\big((N_Tk)^3+N_T^2(N_RK'-1)k^2+N_Tk(N_Tk-1)N_RK'+N_T-1+(N_Tk-1)N_R^2K'^2+(N_RK')(N_RK'-1)+N_{la}(2N_RN_T+(\mu-1)N_T)\big)$
TS	$N_RN_T\mu+\sum_{k=1}^{K-1}N_RN_Tk\eta\mu+K'N_RN_TK\eta$	$N_R(N_T-1)\mu+\sum_{k=1}^{K-1}N_R(N_T-1)k\eta\mu+N_RK'\eta$
Proposed BML	$(KL_c+L_c(L_c-1))QN_RN_T+\mu^KN_R(K+L_c-1)KN_T$	$(KL_c+L_c(L_c-1))(Q-1)N_RN_T+\mu^KN_R(K+L_c-1)(KN_T-1)$
Proposed BPIC	$(KL_c+L_c(L_c-1))QN_RN_T+K\big((N_T(K-1))^3+2N_T^2N_RK'(K-1)^2+N_TN_R^2K'^2(K-1)+(N_RK')^2+\mu N_RK'N_T\big)$	$(KL_c+L_c(L_c-1))(Q-1)N_RN_T+\big((N_T(K-1))^3+N_T^2(N_RK'-1)(K-1)^2+N_T(K-1)(N_T(K-1)-1)N_RK'+N_TN_R^2K'^2(K-1)-N_RK'+N_RK'(N_RK'-1)+\mu N_RK'(N_T-1)\big)$
Proposed BPIC-SIC	$(KL_c+L_c(L_c-1))QN_RN_T+\sum_{k=1}^{K}\big((N_Tk)^3+2N_T^2N_RK'k^2+N_TN_R^2K'^2k+(N_RK')^2+\mu N_RK'N_T\big)$	$(KL_c+L_c(L_c-1))(Q-1)N_RN_T+\sum_{k=1}^{K}\big((N_Tk)^3+N_T^2(N_RK'-1)k^2+N_Tk(N_Tk-1)N_RK'+(N_Tk-1)N_R^2K'^2+N_T-1+(N_RK')(N_RK'-1)+\mu N_RK'(N_T-1)\big)$
Proposed BTS	$(KL_c+L_c(L_c-1))QN_RN_T+N_RN_T\mu+\sum_{k=1}^{K-1}N_RN_Tk\eta\mu+K'N_RN_TK\eta$	$(KL_c+L_c(L_c-1))(Q-1)N_RN_T+N_R(N_T-1)\mu+\sum_{k=1}^{K-1}N_R(N_T-1)k\eta\mu+N_RK'\eta$
Proposed BRCTS	$(KL_c+L_c(L_c-1))QN_RN_T+N_RN_T\mu+\sum_{k=1}^{L_c-1}N_RN_Tk\eta\mu+(K-L_c)N_RN_TL_c\eta\mu+K'N_RKN_T\eta$	$(KL_c+L_c(L_c-1))(Q-1)N_RN_T+N_R(N_T-1)\mu+\sum_{k=1}^{L_c-1}N_R(N_T-1)k\eta\mu+(K-L_c)N_R(N_T-1)L_c\eta\mu+N_RK'\eta$
Proposed BRCTS-SD	$(KL_c+L_c(L_c-1))QN_RN_T+N_RN_T\mu+\sum_{k=1}^{L_c-1}N_RN_Tk\eta_{k-1}\mu+(K-L_c)N_RN_TL_c\eta_{k-1}\mu+K'N_RKN_T\eta_{K-1}$	$(KL_c+L_c(L_c-1))(Q-1)N_RN_T+N_R(N_T-1)\mu+\sum_{k=1}^{L_c-1}N_R(N_T-1)k\eta_{k-1}\mu+(K-L_c)N_R(N_T-1)L_c\eta_{k-1}\mu+N_RK'\eta_{K-1}$

5. Performance evaluation

In this section, the performance of the new methods is evaluated. First, we characterize their computational complexity in terms of the number of multiplications and additions. Next, we assess their BER in different scenarios using computer simulations.

5.1. Computational complexity

Assuming that BEM coefficients are available at the receiver, the computation of $\mathbf{B}_k\mathbf{C}_l$ needs QN_RN_T complex multiplications and $(Q-1)N_RN_T$ complex additions. Thus, for the computation of $\mathbf{G}$, the number of complex multiplications and additions are respectively, $(KL_c+L_c(L_c-1))QN_RN_T$ and $(KL_c+L_c(L_c-1))(Q-1)N_RN_T$.

Based on (13), we should perform $\mu^KN_R(K+L_c-1)KN_T$ complex multiplications and $\mu^KN_R(K+L_c-1)(KN_T-1)$ complex additions in addition to the calculation of $\mathbf{G}$ for the BML method.

Considering the BPIC approach, the computational complexity at each iteration can be obtained as follows. Computation of $\mathbf{\Pi}^{\perp}_{\mathcal{I}_m}$ requires approximately $(N_T(K-1))^3+2N_T^2N_R(K+L_c-1)(K-1)^2+N_TN_R^2(K+L_c-1)^2(K-1)$ complex multiplications and $(N_T(K-1))^3+N_T^2(N_R(K+L_c-1)-1)(K-1)^2+N_T(K-1)(N_T(K-1)-1)N_R(K+L_c-1)+N_TN_R^2(K+L_c-1)^2(K-1)-N_R(K+L_c-1)$ complex additions. For (22), we need $(N_R(K+L_c-1))^2$ complex multiplications and $(N_R(K+L_c-1))(N_R(K+L_c-1)-1)$ complex additions. In addition, $\mu N_R(K+L_c-1)N_T$ complex multiplications and $\mu N_R(K+L_c-1)(N_T-1)$ complex additions should be performed for (19).

Regarding the BPIC-SIC method, the complexity for the $(K-k)$th iteration $(k=0,\cdots,K-1)$ can be computed as follows. For (24) and (25), we need approximately $(N_Tk)^3+2N_T^2N_R(K+L_c-1)k^2+N_TN_R^2(K+L_c-1)^2k$ complex multiplications and $(N_Tk)^3+N_T^2(N_R(K+L_c-1)-1)k^2+N_Tk(N_Tk-1)N_R(K+L_c-1)+(N_Tk-1)N_R^2(K+L_c-1)^2+N_T-1$ complex additions. Moreover, (27) requires $(N_R(K+L_c-1))^2$ complex multiplications and $(N_R(K+L_c-1))(N_R(K+L_c-1)-1)$ complex additions, and (28) needs calculation of $\mu N_R(K+L_c-1)N_T$ complex multiplications and $\mu N_R(K+L_c-1)(N_T-1)$ complex additions.

Considering the BTS approach, except for $\Lambda(\tilde{\mathbf{s}}_0)$ that needs $N_RN_T\mu$ complex multiplications and $N_R(N_T-1)\mu$ complex additions, we need $N_RN_Tk\eta\mu$ complex multiplications and $N_R(N_T-1)k\eta\mu$ complex additions for the computation of (35) for each k. Besides, for (38), we should perform $(K+L_c-1)N_RKN_T\eta$ complex multiplications and $(K+L_c-1)N_R\eta$ complex additions.

The complexity calculation of the BRCTS method is the same as that of the BTS approach except for its cost function for $k>L_c-1$ which needs $N_RN_TL_c\eta\mu$ complex multiplications and $N_R(N_T-1)L_c\eta\mu$ complex additions for each k.

For the BRCTS-SD method, the complexity computation is similar to that of the BRCTS method. The only difference results from $\eta_k\le\eta$, for $k>0$. Thus, the cost function of BRCTS-SD needs $N_RN_TL_c\eta_{k-1}\mu$ complex multiplications and $N_R(N_T-1)L_c\eta_{k-1}\mu$ complex additions for each $k>0$.

In Table 1, the total computational complexities of the proposed methods along with those of PIC, PIC-SIC, PIC-SIC-LaMP, and TS methods are summarized. PIC-SIC-LaMP denotes the method of PIC-SIC followed by the graph-based method called layered message passing (LaMP) developed in [52,53] for slow fading channels. The number of iterations of PIC-SIC-LaMP is shown by N_{la} in this table.

Figs. 2 and 3 illustrate the total computational complexity of the new methods in terms of the number of complex multiplications and additions, respectively (the relevant parameter values are given in the next subsection). For the BRCTS-SD detector, we have shown the average complexity with respect to η_k, which is the number of the valid trial signal vectors falling within the specified radius at the kth step, at the SNR = 20 dB. The numbers of complex multiplications and additions for the BML method, are not shown in these figures as they are too large, and do not help in the comparison. For example for $K=16,32,64$, the numbers of

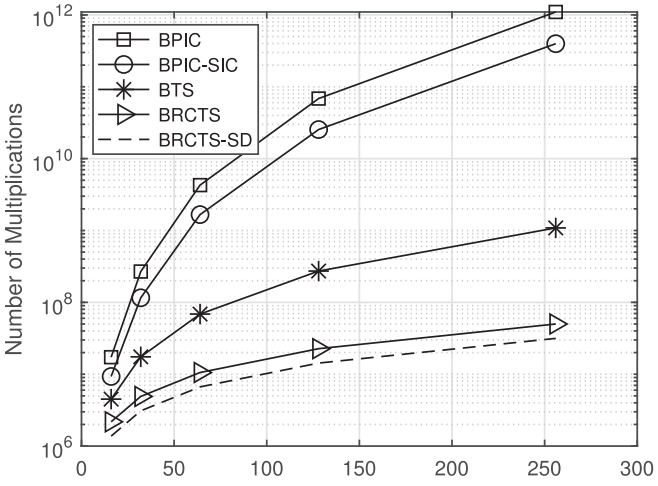

Fig. 2. Number of multiplications versus K for the proposed detectors.

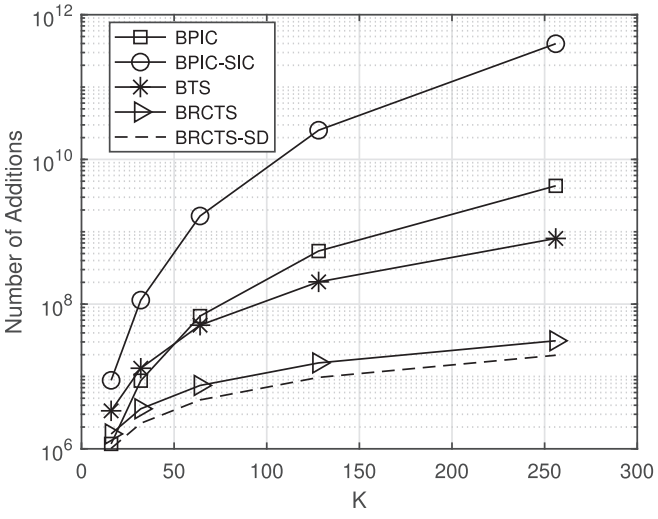

Fig. 3. Number of additions versus K for the proposed detectors.

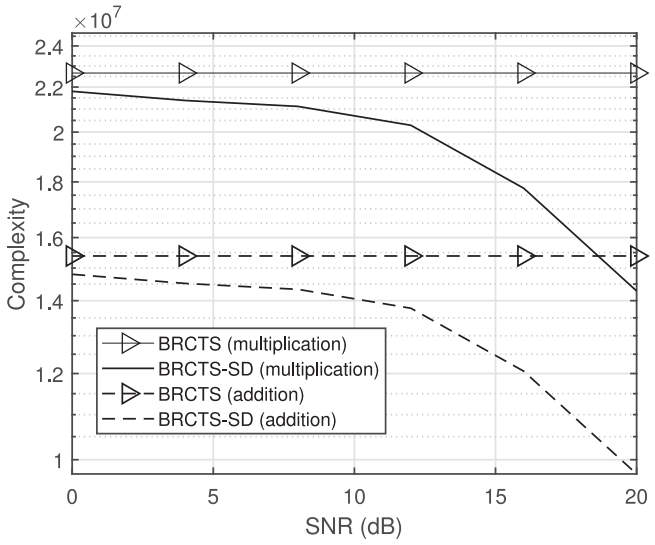

Fig. 4. Number of multiplications and additions versus SNR for the proposed BRCTS and BRCTS-SD detectors.

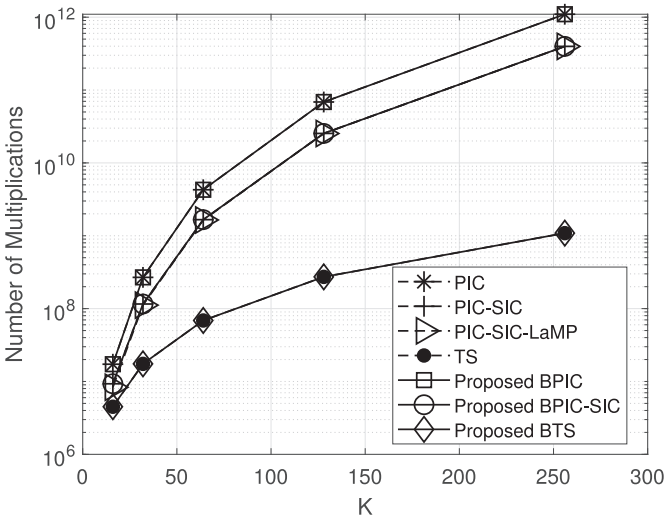

Fig. 5. Number of multiplications versus K for the proposed methods compared with previous methods.

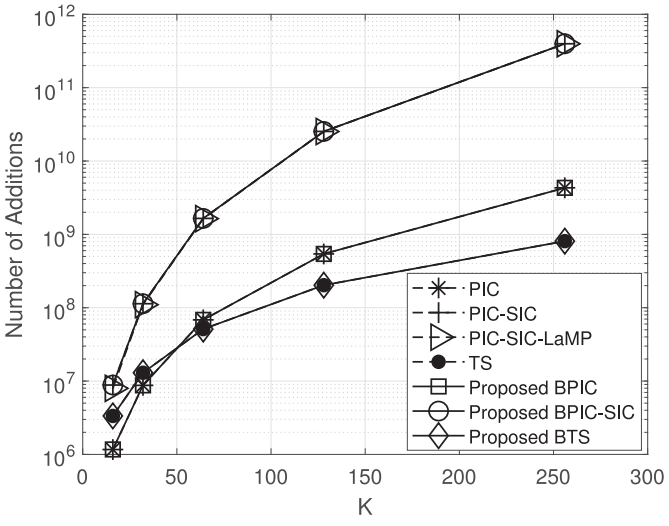

Fig. 6. Number of additions versus K for the proposed methods compared with previous methods.

complex multiplications and additions for BML are 1.74×10^{42}, 2.13×10^{81}, 9.3×10^{158} and 1.71×10^{42}, 2.11×10^{81}, 9.33×10^{158}, respectively. According to these figures, the tree search based methods have significantly lower complexity than the BPIC and BPIC-SIC methods. Moreover, the BRCTS-SD detector has the lowest complexity among the tree-search based methods as it needs to check fewer trial vectors compared with the BTS and BRCTS methods, i.e., $\eta_k \leq \eta$.

In Fig. 4, we have compared the complexity of BRCTS with the average complexity of the BRCTS-SD methods for different values of SNR. Evidently, the complexity of BRCTS-SD is lower than that of BRCTS, and significantly decreases as the SNR increases. The latter observation is due to fact that, with the increase in SNR, the average number of trial vectors that need to be checked (η_k) significantly decreases.

Figs. 5 and 6, respectively illustrate the number of multiplications and additions for the proposed methods and previous PIC, PIC-SIC, PIC-SIC-LaMP, and TS methods. It is observed that the proposed BPIC and BPIC-SIC have approximately the same complexity as the previous PIC, PIC-SIC, and PIC-SIC-LaMP methods. Besides, the proposed BTS method has approximately the same complexity as the TS method, although the new methods lead to notable improvements in BER, as discussed below.

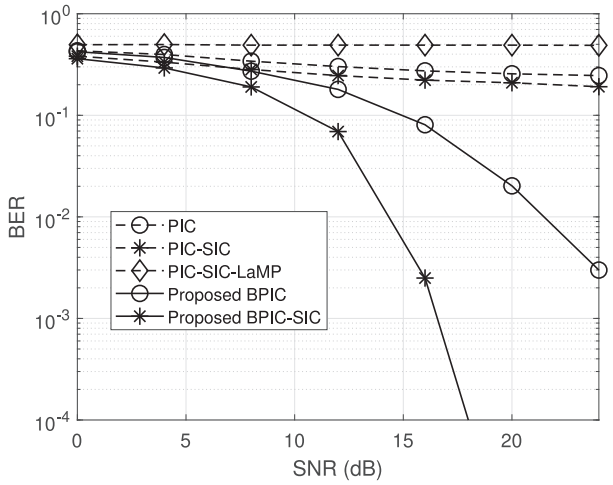

Fig. 7. BER versus SNR for the proposed BPIC and BPIC-SIC detectors compared with the PIC, PIC-SIC, and BPIC-SIC-LaMP detectors.

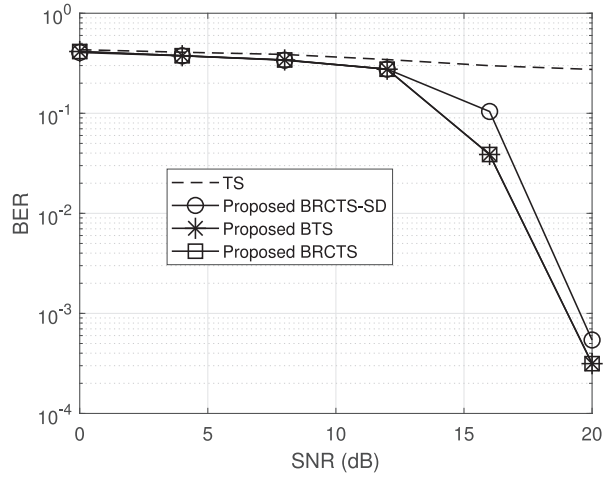

Fig. 8. BER versus SNR for the proposed BTS, BRCTS, and BRCTS-SD detectors compared with the previous tree search-based detector.

5.2. Simulation result

Computer simulations are performed to evaluate the performance of the new methods in DSCs. A SC-GSM system with block size $K = 64$ and zero-padding length of $K_G = 8$ is considered. Unless otherwise stated, the number of transmit and receive antennas are set as $N_T = N_R = 4$, while the number of active antennas is $N_a = 2$. The sampling and carrier frequencies are $f_s = 1.11$ MHz and 1.9 GHz, respectively. The MIMO channel has $L_c = 5$ taps with time spacings of $0.9\mu s$ where the average path gain of the lth tap $(l = 0, 1, \cdots, L_c - 1)$ is $\exp(-\frac{l}{10})$. The channel undergoes Rayleigh fading generated according to the Jake's model [54] with the normalized Doppler frequency of $\frac{f_D}{f_s} = f_D T_s = \frac{0.1}{K}$ corresponding to a mobile speed of 274 km/h. The GCE-BEM is used with $Q = 3$ and $\lambda = 32$ for representing the DSC in our proposed methods. The individual signal symbols at each active antenna are taken from a quadrature amplitude modulation (QAM) constellation with size 8. We assume that the receiver is aware of the BEM coefficients of the DSC, but is not aware of the Jake's true DSC as it can never be attained practically [26]. We also assume that the methods in [17,19,52,53], that are developed for slow fading channels, treat the DSC as if it were a frequency selective channel with no time-variations. In the implementation of the proposed tree search based methods, we set $\eta = 8$.

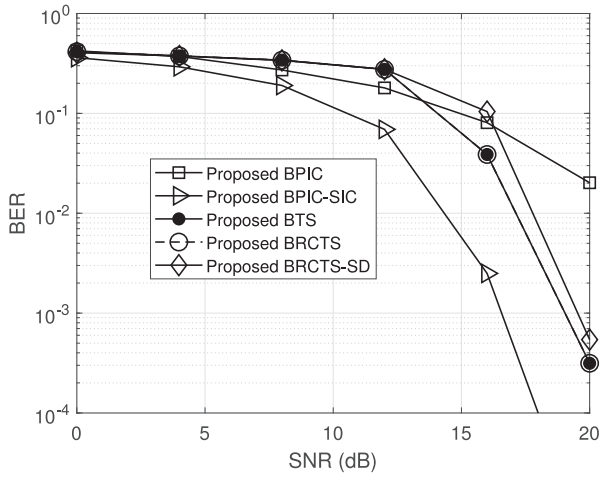

Fig. 9. BER versus SNR for the proposed detectors for $N_T = N_R = 4$, $N_a = 2$.

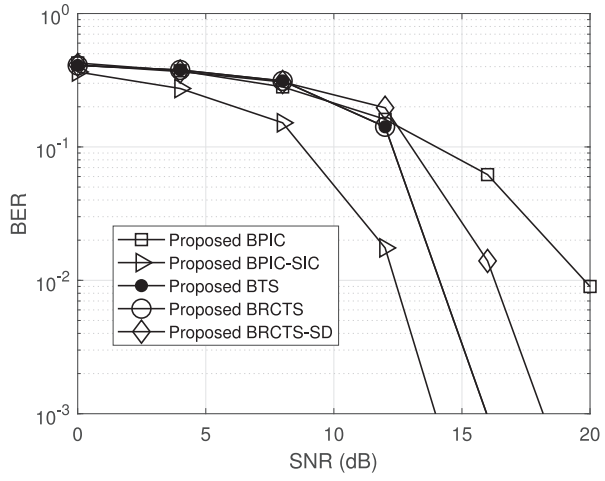

Fig. 10. BER versus SNR for the proposed detectors for $N_T = N_R = 6$ and $N_a = 2$.

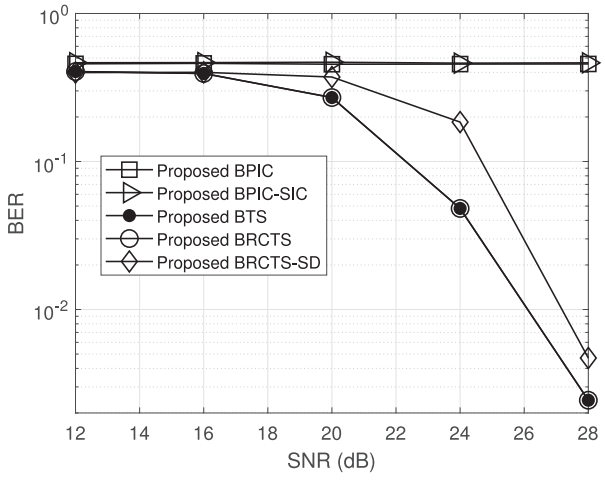

Fig. 11. BER of the proposed detectors for $N_T = 4$, $N_R = 2$ and $N_a = 2$.

In Fig. 7, we have plotted the BER of the proposed BPIC and BPIC-SIC methods along with that of PIC, PIC-SIC, and PIC-SIC-LaMP methods for comparison. Clearly, by considering the time-variations of a DSC, the proposed methods can achieve significantly better performance than the previous ones. Besides, the BPIC-SIC method has considerably lower BER compared with the

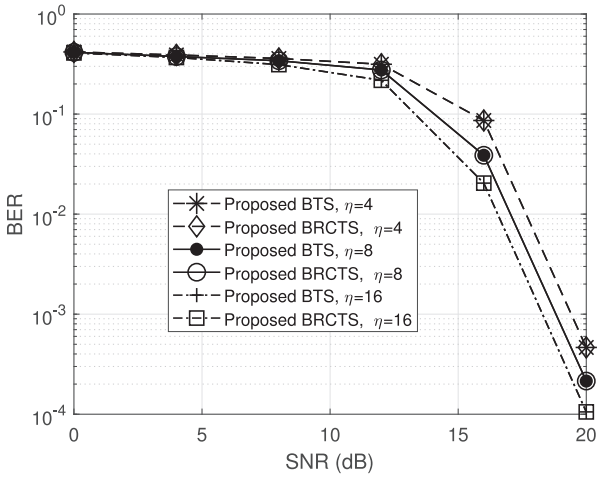

Fig. 12. BER versus SNR for the proposed BTS and BRCTS detectors for different values of η, $N_T = N_R = 4$ and $N_a = 2$.

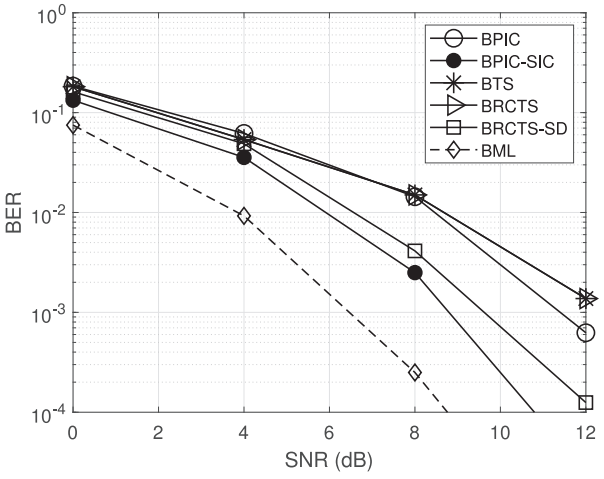

Fig. 13. BER of the proposed BML detector along with other proposed reduced complexity detectors, $N_T = N_R = 2$ and $N_a = 1$.

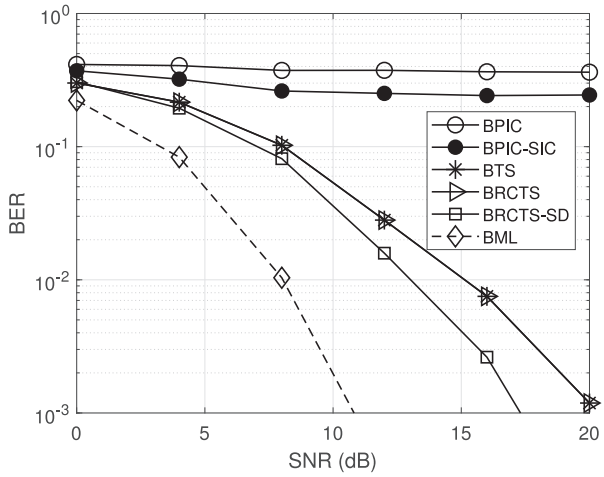

Fig. 14. BER of the proposed BML detector along with other proposed reduced complexity detectors, $N_T = 2$, $N_R = 1$ and $N_a = 1$.

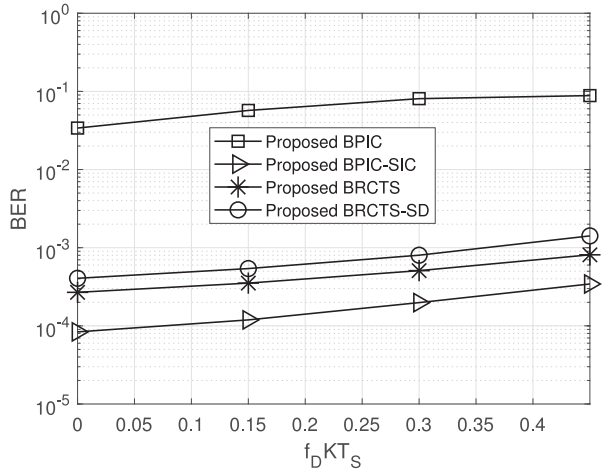

Fig. 15. BER of the proposed detectors for different time-selectivities, $N_T = N_R = 4$ and $N_a = 2$.

BPIC method, as the BPIC-SIC method can more effectively reduce the interference.

Fig. 8, shows the BER of the proposed tree search-based methods along with the tree-search methods in [19]. Again, it is evident that modeling the time-variations of a DSC using BEM can improve the performance compared with the previous tree-search based method whose BER is indicated by "TS" in the figure. Besides, the BRCST method (the reduced complexity method for implementation of the BTS method) has the same performance as BTS, whereas the BRCST-SD method exhibits a slightly higher BER implying that pruning the tree based on the least values of a cost function can be more reliable than pruning based on sphere-decoding. It is worth noting that, as demonstrated in the previous subsection, the BRCST-SD method benefits from lower complexity.

The performance of all of the proposed methods in terms of BER versus SNR for different antenna configurations is shown in Figs. 9–11. In the first two figures, i.e. Figs. 9 and 10, we have $N_T = N_R = 4$ and $N_T = N_R = 6$, respectively. Consequently, the condition $(K + L_c - 1)N_R \geq (K - 1)N_T$ mentioned in Section III for satisfactory performance of the BPIC and BPIC-SIC methods is met. Considering these two figures, it is evident that the proposed BPIC-SIC method has the best performance. However, in the third figure, i.e., Fig. 11, we have $N_T = 4$ and $N_R = 2$, and the above condition is not satisfied, resulting in the poor performance of the BPIC and BPIC-SIC methods. The performance of the proposed tree search-based methods, on the other hand, remains quite good.

In Fig. 12, the BER of proposed BTS and BRCTS methods versus SNR is plotted for different values of η. According to this figure, the performance improves with increasing η as more trial signal vectors are tested for each k, for $k = 1, \cdots, K - 1$.

We compare the performance of the BML method with the other proposed methods in Figs. 13 and 14 where the parameters are as follows: $N_T = 2$, $N_a = 1$, $K = 8$, $T_s = 7.2$ μs. Besides, in Fig. 13, the number of the receive antennas $N_R = 2$ is equal to the number of transmit antennas, whereas in Fig. 14, the number of receive antennas is $N_R = 1$ which is less than the number of transmit antennas. As expected, the BML method has lower BER compared with the other proposed methods. However, since the complexity of the BML method grows exponentially as shown in the previous subsection, except for very simple cases, it remains infeasible in practice. Moreover, when the condition $(K + L_c - 1)N_R \geq (K - 1)N_T$ is not satisfied as in Fig. 14, as discussed before, the proposed BPIC and BPIC-SIC methods do not have satisfactory performance.

Fig. 15 shows the BER performance of the proposed methods for different values of the time selectivity factor $f_d KT_s$. As shown in this figure, the BER slightly increases as the rate of change of the channel increases, but is not overly sensitive to this factor.

In Figs. 16 and 17, the effect of poor channel modeling in terms of the number of basis coefficients Q and basis expansion function is shown respectively. It can be seen that reducing the number

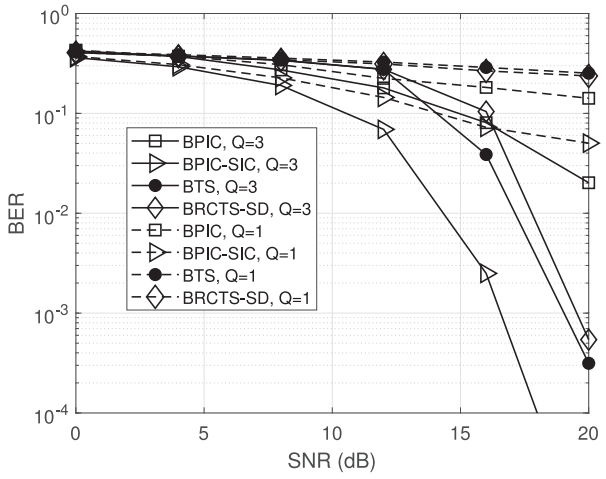

Fig. 16. BER versus SNR for the proposed detectors for $N_T = N_R = 4$, $N_a = 2$ and different values of Q.

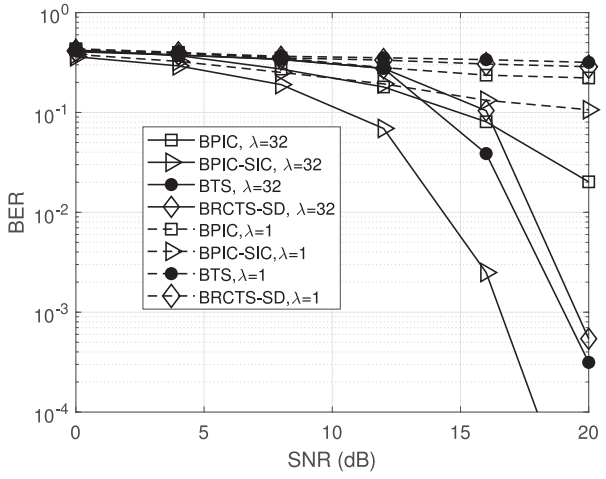

Fig. 17. BER versus SNR for the proposed detectors for $N_T = N_R = 4$, $N_a = 2$, and different values of λ.

of basis coefficients Q, or using a poor choice of basis expansion function corresponding to $\lambda = 1$ in (10) can considerably deteriorate the BER performance.

6. Conclusion

In this paper, we have presented new methods for SC-GSM signal detection under high-mobility situations. Following the representation of a DSC using BEM, the BML detector was first presented, and subsequently, BPIC, BPIC-SIC, BTS, BRCTS and BRCTS-SD methods were introduced aiming at reducing the detection computational complexity. In particular, the proposed BPIC and BPIC method are developed to eliminate the interference between the signals, whereas the proposed BTS, BRCTS, and BRCTS-SD are advanced to restrict the search space and reduce complexity. The performance evaluations of the new methods was performed in terms of computational complexity and BER. The complexity assessments demonstrate that the tree search-based methods have significantly lower complexity than the BPIC-based methods. The BER comparisons show that the new methods considerably improve the performance compared with previous methods.

Declaration of Competing Interests

None.

CRediT authorship contribution statement

Hamed Abdzadeh-Ziabari: Conceptualization, Validation, Methodology, Writing - original draft. **Benoit Champagne:** Resources, Writing - review & editing, Supervision, Funding acquisition.

References

[1] E. Basar, Index modulation techniques for 5g wireless networks, IEEE Commun. Mag. 54 (7) (2016) 168–175, doi:10.1109/MCOM.2016.7509396.
[2] M.D. Renzo, H. Haas, Space shift keying (SSK) MIMO over correlated rician fading channels: performance analysis and a new method for transmit-diversity, IEEE Trans. Commun. 59 (1) (2011) 116–129, doi:10.1109/TCOMM.2011.111710.090775.
[3] R. Mesleh, H. Haas, C.W. Ahn, S. Yun, Spatial modulation-a new low complexity spectral efficiency enhancing technique, in: Int. Conf. on Communications and Networking, 2006, pp. 1–5, doi:10.1109/CHINACOM.2006.344658.
[4] R.Y. Mesleh, H. Haas, S. Sinanovic, C.W. Ahn, S. Yun, Spatial modulation, IEEE Trans. Veh. Technol. 57 (4) (2008) 2228–2241, doi:10.1109/TVT.2007.912136.
[5] J. Jeganathan, A. Ghrayeb, L. Szczecinski, A. Ceron, Space shift keying modulation for MIMO channels, IEEE Trans. Wire. Commun. 8 (7) (2009) 3692–3703, doi:10.1109/TWC.2009.080910.
[6] E. Basar, U. Aygolu, E. Panayirci, H.V. Poor, Space-time block coded spatial modulation, IEEE Trans. Commun. 59 (3) (2011) 823–832, doi:10.1109/TCOMM.2011.121410.100149.
[7] V. Tarokh, H. Jafarkhani, A.R. Calderbank, Space-time block codes from orthogonal designs, IEEE Trans. Inform. Theory 45 (5) (1999) 1456–1467, doi:10.1109/18.771146.
[8] A. Younis, N. Serafimovski, R. Mesleh, H. Haas, Generalised spatial modulation, in: Conference Record of the Forty Fourth Asilomar Conference on Signals, Systems and Computers, 2010, pp. 1498–1502, doi:10.1109/ACSSC.2010.5757786.
[9] J. Wang, S. Jia, J. Song, Generalised spatial modulation system with multiple active transmit antennas and low complexity detection scheme, IEEE Trans. Wire. Commun. 11 (4) (2012) 1605–1615, doi:10.1109/TWC.2012.030512.111635.
[10] S. Sugiura, S. Chen, L. Hanzo, Generalized space-time shift keying designed for flexible diversity-, multiplexing- and complexity-tradeoffs, IEEE Trans. Wire. Commun. 10 (4) (2011) 1144–1153, doi:10.1109/TWC.2011.012411.100065.
[11] B. Hassibi, B.M. Hochwald, High-rate codes that are linear in space and time, IEEE Trans. Inform. Theory 48 (7) (2002) 1804–1824, doi:10.1109/TIT.2002.1013127.
[12] G.J. Foschini, Layered space-time architecture for wireless communication in a fading environment when using multi-element antennas, Bell Labs Tech. J. 1 (2) (1996) 41–59.
[13] S. Sugiura, L. Hanzo, Single-RF spatial modulation requires single-carrier transmission: frequency-domain turbo equalization for dispersive channels, IEEE Trans. Veh. Technol. 64 (10) (2015) 4870–4875, doi:10.1109/TVT.2014.2370679.
[14] L. Xiao, Y. Xiao, Y. Zhao, P. Yang, M.D. Renzo, S. Li, W. Xiang, Time-domain turbo equalization for single-carrier generalized spatial modulation, IEEE Trans. Wire. Commun. 16 (9) (2017) 5702–5716, doi:10.1109/TWC.2017.2713777.
[15] L. He, J. Wang, J. Song, A priori information-aided iterative equalization: anovel approach for single-carrier spatial modulation in dispersive channels, IEEE Trans. Veh. Technol. 66 (5) (2017) 4448–4452, doi:10.1109/TVT.2016.2598846.
[16] P.Y. et al, Single-carrier SM-MIMO: a promising design for broadband large-scale antenna systems, IEEE Commun. Surv. Tut. 18 (3) (2016) 1687–1716, doi:10.1109/COMST.2016.2533580.
[17] R. Rajashekar, K.V.S. Hari, L. Hanzo, Spatial modulation aided zero-padded single carrier transmission for dispersive channels, IEEE Trans. Commun. 61 (6) (2013) 2318–2329, doi:10.1109/TCOMM.2013.043013.130011.
[18] F. Yao, J. Zheng, J. Chen, Reduced-complexity partial interference cancellation receiver in spatial modulation aided zero-padded single carrier transmission, in: Int. Conf. on Wireless Communications Signal Processing (WCSP), 2015, pp. 1–5, doi:10.1109/WCSP.2015.7341009.
[19] L. Xiao, L. Dan, Y. Zhang, Y. Xiao, P. Yang, S. Li, A low-complexity detection scheme for generalized spatial modulation aided single carrier systems, IEEE Commun. Lett. 19 (6) (2015) 1069–1072, doi:10.1109/LCOMM.2015.2404444.
[20] L. Xiao, P. Yang, Y. Zhao, Y. Xiao, J. Liu, S. Li, Low-complexity tree search-based detection algorithms for generalized spatial modulation aided single carrier systems, in: IEEE Int. Conf. on Communications (ICC), 2016, pp. 1–6, doi:10.1109/ICC.2016.7511399.
[21] B. Gong, L. Gui, Q. Qin, X. Ren, W. Chen, Block distributed compressive sensing-based doubly selective channel estimation and pilot design for large-scale MIMO systems, IEEE Trans. Veh. Technol. 66 (10) (2017) 9149–9161, doi:10.1109/TVT.2017.2715345.
[22] J. Huang, S. Zhou, J. Huang, C.R. Berger, P. Willett, Progressive inter-carrier interference equalization for OFDM transmission over time-varying underwater acoustic channels, IEEE J. Select. Topics Sig. Process. 5 (8) (2011) 1524–1536, doi:10.1109/JSTSP.2011.2160040.
[23] Y. Li, X. Sha, F. Zheng, K. Wang, Low complexity equalization of HCM systems with DPFFT demodulation over doubly-selective channels, IEEE Sig. Process. Lett. 21 (7) (2014) 862–865, doi:10.1109/LSP.2014.2311128.
[24] I. Barhumi, G. Leus, M. Moonen, Time-varying FIR decision feedback equalization of doubly-selective channels, in: Proc. IEEE Global Telecommunications Conference, 4, 2003, pp. 2263–2268, doi:10.1109/GLOCOM.2003.1258638.

[25] I. Barhumi, G. Leus, M. Moonen, Time-domain and frequency-domain per-tone equalization for OFDM over doubly selective channels, Signal Processing 84 (11) (2004) 2055–2066, doi:10.1016/j.sigpro.2004.07.016. Special Section Signal Processing in Communications
[26] I. Barhumi, G. Leus, M. Moonen, Time-varying FIR equalization for doubly selective channels, IEEE Trans. Wire. Commun. 4 (1) (2005) 202–214, doi:10.1109/TWC.2004.840204.
[27] T. Hrycak, S. Das, G. Matz, H.G. Feichtinger, Low complexity equalization for doubly selective channels modeled by a basis expansion, IEEE Trans. Sig. Process. 58 (11) (2010) 5706–5719, doi:10.1109/TSP.2010.2063426.
[28] K. Zhong, Y. Wu, S. Li, Signal detection for ofdm-based virtual mimo systems under unknown doubly selective channels, multiple interferences and phase noises, IEEE Trans. Wireless Commun. 12 (10) (2013) 5309–5321, doi:10.1109/TWC.2013.090413.130271.
[29] F. Pea-Campos, R. Parra-Michel, V. Kontorovich, MIMO Multicarrier transmission over doubly selective channels with virtual trajectories receiver, IEEE Trans. Veh. Technol. 68 (10) (2019) 9330–9338, doi:10.1109/TVT.2019.2934693.
[30] H. Abdzadeh-Ziabari, B. Champagne, Novel detection methods for zero-padded single carrier spatial modulation in doubly selective channels, in: IEEE International Conference on Acoustics, Speech and Signal Processing (ICASSP), 2019, pp. 4704–4708, doi:10.1109/ICASSP.2019.8682446.
[31] G.B. Giannakis, C. Tepedelenlioglu, Basis expansion models and diversity techniques for blind identification and equalization of time-varying channels, Proc. IEEE 86 (10) (1998) 1969–1986, doi:10.1109/5.720248.
[32] H.A. Cirpan, M.K. Tsatsanis, Maximum likelihood blind channel estimation in the presence of doppler shifts, IEEE Trans. Sig. Process. 47 (6) (1999) 1559–1569, doi:10.1109/78.765125.
[33] G. Leus, On the estimation of rapidly time-varying channels, in: European Signal Processing Conference, 2004, pp. 2227–2230.
[34] D.K. Borah, B.T. Hart, Frequency-selective fading channel estimation with a polynomial time-varying channel model, IEEE Trans. Commun. 47 (6) (1999) 862–873, doi:10.1109/26.771343.
[35] M. Visintin, Karhunen-Loeve expansion of a fast Rayleigh fading process, Electron. Lett. 32 (18) (1996), doi:10.1049/el:19961128. 1712
[36] H. Abdzadeh-Ziabari, W. Zhu, M.N.S. Swamy, Joint maximum likelihood timing, frequency offset, and doubly selective channel estimation for OFDM systems, IEEE Trans. Veh. Technol. 67 (3) (2018) 2787–2791, doi:10.1109/TVT.2017.2728008.
[37] Z. Tang, R.C. Cannizzaro, G. Leus, P. Banelli, Pilot-assisted time-varying channel estimation for OFDM systems, IEEE Trans. Sig. Process. 55 (5) (2007) 2226–2238, doi:10.1109/TSP.2007.893198.
[38] K. Muralidhar, K.H. Li, A low-complexity kalman approach for channel estimation in doubly-selective OFDM systems, IEEE Sig. Process. Lett. 16 (7) (2009) 632–635.
[39] I. Barhumi, M. Moonen, MLSE And MAP equalization for transmission over doubly selective channels, IEEE Trans. Veh. Technol. 58 (8) (2009) 4120–4128.
[40] L. Song, J.K. Tugnait, Doubly-selective fading channel equalization: acomparison of the kalman filter approach with the basis expansion model-based equalizers, IEEE Trans. Wire. Commun. 8 (1) (2009) 60–65.
[41] T. Cui, C. Tellambura, Y. Wu, Low-complexity pilot-aided channel estimation for OFDM systems over doubly-selective channels, in: IEEE Int. Conf. on Communications (ICC), 3, 2005, pp. 1980–1984, doi:10.1109/ICC.2005.1494685.
[42] S. Hou, C.C. Ko, Intercarrier interference suppression for OFDMA uplink in time- and frequency-selective fading channels, IEEE Trans. Veh. Technol. 58 (6) (2009) 2741–2754, doi:10.1109/TVT.2008.2010550.
[43] H. Hijazi, L. Ros, Polynomial estimation of time-varying multipath gains with intercarrier interference mitigation in OFDM systems, IEEE Trans. Veh. Technol. 58 (1) (2009) 140–151, doi:10.1109/TVT.2008.923653.
[44] J.K. Tugnait, S. He, Doubly-selective channel estimation using data-dependent superimposed training and exponential basis models, IEEE Trans. Wire. Commun. 6 (11) (2007) 3877–3883.
[45] T. Whitworth, M. Ghogho, D. McLernon, Optimized training and basis expansion model parameters for doubly-selective channel estimation, IEEE Trans. Wirel. Commun. 8 (3) (2009) 1490–1498, doi:10.1109/TWC.2009.080364.
[46] K. Zhong, X. Lei, S. Li, Wiener filter for basis expansion model based channel estimation, IEEE Commun. Lett. 15 (8) (2011) 813–815, doi:10.1109/LCOMM.2011.060811.110521.
[47] X. Guo, X. Xia, On full diversity space time block codes with partial interference cancellation group decoding, IEEE Trans. Inf. Theory 55 (10) (2009) 4366–4385, doi:10.1109/TIT.2009.2027502.
[48] W. Liu, N. Wang, M. Jin, H. Xu, Denoising detection for the generalized spatial modulation system using sparse property, IEEE Commun. Lett. 18 (1) (2014) 22–25, doi:10.1109/LCOMM.2013.111413.131722.
[49] C. Wang, P. Cheng, Z. Chen, J.A. Zhang, Y. Xiao, L. Gui, Near-ml low-complexity detection for generalized spatial modulation, IEEE Commun. Lett. 20 (3) (2016) 618–621, doi:10.1109/LCOMM.2016.2516542.
[50] A. Younis, S. Sinanovic, M.D. Renzo, R. Mesleh, H. Haas, Generalised sphere decoding for spatial modulation, IEEE Trans. Commun. 61 (7) (2013) 2805–2815, doi:10.1109/TCOMM.2013.061013.120547.
[51] B. Hassibi, H. Vikalo, On the sphere-decoding algorithm i. expected complexity, IEEE Trans. Sig. Process. 53 (8) (2005) 2806–2818, doi:10.1109/TSP.2005.850352.
[52] T. Lakshmi Narasimhan, A. Chockalingam, On the capacity and performance of generalized spatial modulation, IEEE Commun. Lett. 20 (2) (2016) 252–255, doi:10.1109/LCOMM.2015.2497255.
[53] S. Fan, Y. Xiao, L. Xiao, P. Yang, R. Shi, K. Deng, Improved layered message passing algorithms for large-scale generalized spatial modulation systems, IEEE Wire. Commun. Lett. 7 (1) (2018) 66–69, doi:10.1109/LWC.2017.2753801.
[54] W.C. Jakes, D.C. Cox, Microwave mobile communications, Wiley-IEEE Press, 1994.